



**DESIGN CONSIDERATIONS FOR A WATER TREATMENT SYSTEM
UTILIZING ULTRA-VIOLET LIGHT EMITTING DIODES**

THESIS

Michael J Spencer, Captain, USAF

AFIT-ENV-14-M-58

**DEPARTMENT OF THE AIR FORCE
AIR UNIVERSITY**

AIR FORCE INSTITUTE OF TECHNOLOGY

Wright-Patterson Air Force Base, Ohio

DISTRIBUTION STATEMENT A.
APPROVED FOR PUBLIC RELEASE; DISTRIBUTION UNLIMITED.

The views expressed in this thesis are those of the author and do not reflect the official policy or position of the United States Air Force, Department of Defense, or the United States Government. This material is declared a work of the U.S. Government and is not subject to copyright protection in the United States.

AFIT-ENV-14-M-58

DESIGN CONSIDERATIONS FOR A WATER TREATMENT SYSTEM
UTILIZING ULTRA-VIOLET LIGHT EMITTING DIODES

THESIS

Presented to the Faculty

Department of Systems and Engineering Management

Graduate School of Engineering and Management

Air Force Institute of Technology

Air University

Air Education and Training Command

In Partial Fulfillment of the Requirements for the
Degree of Master of Science in Engineering Management

Michael J. Spencer, BS

Captain, USAF

March 2014

DISTRIBUTION STATEMENT A:

APPROVED FOR PUBLIC RELEASE; DISTRIBUTION UNLIMITED.

**DESIGN CONSIDERATIONS FOR A WATER TREATMENT SYSTEM
UTILIZING ULTRA-VIOLET LIGHT EMITTING DIODES**

Michael J. Spencer, BS

Captain, USAF

Approved:

<u>//Signed//</u> Dr. Michael E. Miller, PhD (Chairman)	<u>13MAR2014</u> Date
<u>//Signed//</u> Leeann Racz, Lt Col, USAF, PhD (Member)	<u>13MAR2014</u> Date
<u>//Signed//</u> Dr. Michael R. Grimaila, PhD, CISM, CISSP (Member)	<u>13MAR2014</u> Date
<u>//Signed//</u> Dr. Alfred E. Thal Jr., PhD (Member)	<u>13MAR2014</u> Date

ABSTRACT

UV LED technology is in its infancy and research as it applies to UV water treatment is required to advance knowledge for practical application. This thesis focused on two subjects. First, the design, fabrication, and operation of a water treatment reaction system utilizing Ultra-Violet (UV) Light Emitting Diodes (LEDs). Second, the measurement of UV LED output angle in water which is necessary to support future reactor designs. Several characteristics of the LED-water interface were revealed which impacted the effectiveness of the vessel including; UV dose requirements, LED wavelength, photon dispersion geometry, LED placement, optical path efficiency, vessel material, and electronic control system. The reactor vessel design balanced optimal characteristics with experiment design flexibility, fabrication speed, and procurement considerations. Expedient construction was required to permit laboratory exploration performed by other researchers studying bacterial spore disinfection, an advanced oxidation process, and UV LED output wavelength and intensity observations. Two reactor vessels and three electronic boards were completed and modified as the research matured. Next, the UV LED output angle in air and water was measured. The conclusions of the literature review, practical application, and output angle calculations led to future design considerations for a UV LED, water reaction vessel, and electronic control system.

Acknowledgments

First and foremost, I would like to thank Bethany, Madelyn, and Nathan for their support, renditions of “Frozen” songs, and daily facetious additions to my workload.

Second, the leadership and guidance from Lt Col Racz, Dr. Miller, and Dr. Grimaila was critical to the success of the efforts of our research team.

I would also like to thank my teammates: Maj Tho Tran, Capt Kelsey Duckworth, Capt Chris Bates, and Capt John Richwine. This research has been a learning experience and it would not have been possible without them.

Lastly, I need to acknowledge my fellow classmates of 14M GEM and our study of George Simplex and his method as it pertains to the optimization of manufacturing hot tubs.

//Signed/mjs/13Mar14//
Michael J. Spencer

Table of Contents

	Page
ABSTRACT.....	iv
Table of Contents	vi
List of Figures.....	vii
List of Tables.....	ix
I. INTRODUCTION	1
General Issue.....	1
Problem Statement.....	3
Investigative Questions.....	3
Methodology.....	3
Assumptions/Limitations	4
II. INITIAL DESIGN CONSIDERATIONS	5
Overview.....	5
LED Wavelength.....	6
UV Dose Requirements	8
Dispersion Pattern.....	9
Optical Path Design	14
Vessel Material.....	20
LED Placement.....	22
III. SYSTEM DESIGN, OPERATION, AND MODIFICATION.....	24
LED Control Components	26
Construction and Operation	29
LED and LED Plate Modifications.....	32
Reactor Vessel Modifications	33
LED Drive Board Modifications	34
IV. CHARACTERIZATION OF LED OUTPUT IN WATER.....	38
Introduction.....	38
Methodology.....	38
Air Data Analysis.....	41
Water Measurement Analysis	44
V. CONCLUSION	47
Summary.....	47
Future Design Considerations.....	50
Recommendations for Action	57
APPENDIX: LED OUTPUT ANGLE PLOTS.....	59

List of Figures

	Page
Figure 1. Optical power relationship with temperature.....	9
Figure 2. Variety of LED Lens emission geometry.....	10
Figure 3. SETi UV TO39 Flat Window lens power intensity shape in air.....	11
Figure 4. Light from LED substrate through silica window to air and water, figure not to scale.....	12
Figure 5. Diagram of Snell's Law as it applies to the UV LED window (Medium 1) and air or water (Medium 2).....	12
Figure 6. Refraction angle dependence on angle of incidence due to internal reflection of a material with $n=1.5$ from which light propagates into a gas with $n=1$. Refraction angle greater than 90 degrees denotes the light is internally reflected inside material 1 versus passing into material 2.....	16
Figure 7. Aluminum Reflectance and discussion. The line depicts the approximate position of the wavelengths of interest.....	20
Figure 8. Optimized circle packing within a circle geometries: 7, 12, and 19 circles.....	23
Figure 9. Initial apparatus exploded schematic without flow through pipes shown. Single LED hole shown in left plate.....	24
Figure 10. Completed initial reaction vessel; three inch diameter and three inch length main pipe, one inch diameter flow through pipes all made of sanitary, food-grade finish 316 stainless steel pipe, final polishing via electro-polish process.....	25
Figure 11. USB board made by Measurement Computing.....	26
Figure 12. LED Drive Board.....	28
Figure 13. LED system set up as a batch design with flow through pipes sealed and mounted on an orbital shaker.....	30
Figure 14. Flow through reactor system with silicone hose connecting to a UV Vis measurement device.....	31
Figure 15. Captain Christopher Bates' LED measurement system utilizing the LED drive board with Labsphere air and water measurement vessels.....	31
Figure 16. Single LED plate and seven LED plate.....	32
Figure 17. Aluminum heat sink bracket.....	33
Figure 18. Reactor vessel with flow through pipe sealed.....	34
Figure 19. Input voltage multiplying OPAMP schematic and diagram.....	35
Figure 20. Variable resistors and multiplying OPAMP board added to the original LED drive board.....	37
Figure 21. Diagram of the plastic sheet mounted on the water side of the tank.....	39
Figure 22. Diagram of the LED geometry output measuring device.....	40

Figure 23. LED water output through quantum dot sheet in white light (left) and dark room conditions.....	41
Figure 24. Example output comparison between measured (squares) and predicted angle (triangles).....	42
Figure 25. Example water measurement showing distinct border between light and dark (left) and air measurement (right).....	45
Figure 26. Potential reflectors for inside the LED.....	52
Figure 27. Example modeled cross-section of UV LED output dispersion in water; angle in degrees, intensity normalized.....	53
Figure 28. Modeled LED output inside a three inch reflective pipe vessel.....	54
Figure 29. Single source flow through reactor vessel cross-section.....	55
Figure 30. Multiple LED arrangement with interlocking emission patterns.....	55
Figure 31. Square wave, triangular, and square pulse with constant current.....	57

List of Tables

	Page
Table 1. Purchased LED Specifications.....	6
Table 2. Example inspection report of LED output.	7
Table 3. Internal angles of the fused silica-nitrogen gas interface and critical angles of internal reflection in silica-air and silica-water interface. Angles are in degrees.....	17
Table 4. Material reflectivity, calculated with Equation 3.	18
Table 5. Measured LED output angles (degrees) in air and water output prediction.	43
Table 6. Measured LED output angles (degrees) in water and difference with water output prediction.	45

List of Equations

	Page
Equation 1. Snell's Law	13
Equation 2. Reflectivity.....	18
Equation 3. Ohm's Law	29
Equation 4. Amplification Ratio	35
Equation 5. Predicted Diameter of Output.....	42

DESIGN CONSIDERATIONS FOR A WATER TREATMENT SYSTEM UTILIZING ULTRA-VIOLET LIGHT EMITTING DIODES

I. INTRODUCTION

General Issue

Light-Emitting-Diode (LED) technology has been in use for decades and great strides have been made in the production of highly efficient, long-lived, high power visible light LED systems (Lenk and Lenk, 2010). These devices have only recently been able to produce energy in the Ultra-Violet (UV) wavelength range (Taniyasu, et al, 2005). Water treatment systems have used UV wavelength fluorescent bulbs for decades (Spelph, 2008) but have only recently started using UV LEDs. Aquionics in Erlanger, KY was among the first companies to utilize UV LEDs in the UV C band (200-300 nm wavelength) to treat water with a flow rate of 0.5 gallons per minute (Aquionics, 2013). Tube-type mercury fluorescent bulb technology is mature enough to service municipality-sized disinfection systems, with flow rates in the millions of gallons per day (Aquionics, 2012). Highly developed systems are available from several manufacturers. For example, the Aquionics municipal flow-through systems use quartz sleeves to house fluorescent light bulbs located within the water treatment chamber and wipers to clean the sleeve to reduce optical loss. These designs utilize computational fluid dynamics models optimize the geometric placement of the bulbs with respect to the water flow (Spelph, 2008). UV fluorescent-type bulbs have also been applied in smaller applications, such as residential hot tubs (Spectralight, 2013).

Unfortunately, fluorescent bulbs are energy intensive, expensive, and fragile. They also have a short lifespan, and they contain mercury. Should UV LED technology progress similarly to visible light LEDs, they should overcome many of the negative attributes of fluorescent bulbs. It is also anticipated that UV LED technology will mature faster than visible wavelength LEDs as the industry will be able to utilize knowledge gained from decades of LED development. The potential mechanical robustness and energy efficiency advantages of a future LED-based UV water treatment system are of interest to the United States Air Force, Department of Defense, and United States Environmental Protection Agency. For these reasons, this research focused on developing a UV LED based water treatment system to be used as a basis to further the knowledge of this capability.

The UV LED water treatment system created and modified for this thesis enabled other researchers to determine the effectiveness of UV LEDs in various aspects of a UV water treatment system. Two other team members investigated the efficiency of the reaction by pulse driving the LED output to disinfect bacterial spores (Tran, 2014) and to create hydroxyl radicals with an advanced oxidation process which can oxidize chemical compounds (Duckworth, 2014). Two additional theses involved creation of a computer model for predicting the radiation dose at any three dimensional point in the reactor (Richwine, 2014) and for measuring the magnitude of the UV LED power output and UV reflectivity of materials in both air and water (Bates, 2014). This investigation continued by examining the UV emission angle from the UV LED in water and exploring potential characteristics which would enhance the effectiveness of the system.

Problem Statement

Traditional water treatment methods utilizing UV light are well defined, but are fundamentally different than LEDs in the manner that photons are emitted. Furthermore, the application of UV LED technology to water treatment is in its infancy phase. Therefore, this thesis endeavors to increase the knowledge base of applying UV LED technology to a flowing water treatment reactor system.

Investigative Questions

To resolve the problem, this thesis strives to answer the following questions:

What characteristics should be considered at the UV LED-water interface and water-reactor vessel interface when designing a reactor?

What is the UV LED energy output geometry in water and how can the reactor geometry be optimized accordingly?

Methodology

This research began with a literature review to obtain pertinent characteristics of UV light, UV LEDs, vessel materials, and vessel geometry. Preliminary investigation formed the basis for an initial reactor design. Materials for this reactor were quickly procured and the reactor was constructed for use by the other researchers. The electronic control circuit board was designed by the faculty team and was constructed by this researcher. The initial system was fielded to the research team and tailored as the

research progressed to meet the design of their experiments. Meanwhile, the UV LED output geometry in water was predicted by applying optical laws to the manufacturer's specified output angle and measurements of the output in air. The three dimensional output geometry in water was then measured. Results from the in-depth investigation, output angle measurement, and lessons learned from the practical application were developed into guidelines for future system designs.

Assumptions/Limitations

UV LEDs are a new technology and, therefore, have several less than ideal scientific properties. As discovered during this project, the individual UV LEDs vary significantly in optical output as a function of electrical input, which does not allow the team to create accurate and precise experiment predictions and significantly increases error in results. Controls must be developed to accurately manage the variability while operating several UV LEDs at the same time. There are only a few manufacturers of UV LEDs, limiting options for selection of components. The electrical control design is one of a kind, presenting several obstacles to practical operation and troubleshooting which are normally not present using commercial, off-the-shelf products. The initial system was completed expeditiously to accommodate time for experimentation by the research team and, therefore, could have incorporated more effective attributes discovered after the fact. Lastly, unpredicted variables and unforeseen issues are common when conducting physical research, and overcoming equipment nuances consumed an inordinate amount of time and resources.

II. INITIAL DESIGN CONSIDERATIONS

Overview

While fluorescent-based UV technology has become commercially viable, the advent of UV-LED technology has not gone unnoticed. Initial LED-based products with flow rates as high as 0.5 gallons per minute and at a dose of 40 mJ/cm² have become commercially available (Aquionics, 2013). This technology is developing at such a pace that commercial LED-based products were not available mere months prior to the start of this research.

An UV LED system would require only a few key components: the LEDs, electronic controls, the water pump for flow through experiments, and the reaction vessel. The LEDs, water pump, and initial electronic control system were chosen by the faculty before this research was started. The reaction vessel had various design requirements. Among these was the requirement that the reactor must be capable of a 5 mL/min flow rate for initial experiments, and allow higher flow rates as experimentation progressed. Further, the vessel must be flexible for use in both water disinfection and oxidation research.

The following system characteristics were investigated: LED wavelength, UV dose requirements, dispersion geometry, LED placement, optical path, vessel material, and LED control components. Each of these characteristics is described in the subsequent sections.

LED Wavelength


The wavelength of UV light was dependent on the purpose. The UV Pearl commercial off-the-shelf water disinfection unit utilizes 275 (+/- 12) nm wavelength LEDs (Aquionics, 2013). An experiment to re-use waste water as farm irrigation utilized 280 and 265 nm LEDs, one each, with a 14 cm crystallization dish containing 250 mL of affluent and radiated for 30 minutes (Chevremont, et al, 2006). Watts and Linden (2008) used calibrated UV bulbs outputting energy at the 254 nm wavelength for oxidation. Major Tran determined that 268 nm is optimum for disinfection of the spores of interest (Tran, 2014). Wavelengths of 260 nm and 270 nm are similar to industry use for UV fluorescent bulb type water disinfection systems (Aquionics, 2013). Shorter wavelength LEDs (240 nm) were shown to be more effective at creating hydroxyl radicals for oxidation (Watts and Linden, 2008). However the use of LEDs at this wavelength may prove to be difficult due to the significantly lower LED UV output of that specific wavelength, as shown in Table 1, and a much greater power requirement to create hydroxyl radicals. However, for this research, it was decided that the disinfection treatment should utilize an LED with a wavelength closest to 268 nm and the oxidation treatment should utilize a 240 nm LED (Duckworth, 2014; Tran, 2014). Both were available from the selected vendor, Sensor Electronic Technology, Inc (S-ETi), located in Columbia, South Carolina.

Table 1. Purchased LED Specifications (S-ETi, 2012)

	Wavelength (nm)	Optical Power (mW)		Lens
		Minimum	Typical	
UVTOP240TO39FW	240	30	70	Flat
UVTOP270TO39BL	270	360	600	Ball
UVTOP270TO39FW	270	480	800	Flat
UVTOP260TO39FW	260	180	300	Flat

At the start of this research, UV LEDs were available from only a single commercial source. Sensor Electronic Technology, Inc., located in Colombia, South Carolina originally developed UV LEDs under the direction of the Defense Advanced Research Projects Agency. Since that time, this manufacturer has commercialized a range of UV LEDs with wavelengths varying from 240 to 360 nm. Although these LEDs are low power devices, useful primarily in sensing applications, this thesis endeavored to apply them to water treatment. Amperage of these devices was limited to 200 mA at a pulsed forward current of 1% duty factor and 1 kHz frequency. Maximum operational temperature was 55 degrees Celsius, with optimal efficiency and lifetime below 20 degrees Celsius. Output power tolerance was claimed to be $\pm 10\%$ optical power. Later purchases of UV LEDs included model UVTOP265TO39FW, which had a wavelength closer to the desired 268 nm. The optical output for each LED was measured at 20 mA forward amperage by S-ETi, as shown in Table 2 (S-ETi, 2013). Knowing the actual optical output of an LED for a given electrical input can predict an approximate dose.

Table 2. Example inspection report of LED output (SETi, 2013)

		QC Inspection Report						
		Customer	AFIT		Date	3/26/2013	PO #	030813DL
		Part #	UVTOP	240	TO39	FW	Box #	0
		Tested	CWG				Test ID	FT - it.1
#	Voltage, V	Current, mA	Power*, W	Peak Wave, nm	HB, nm	PSV*, W / nm		Date / Time
S36	7.138903	20.00	1.74E-04	247.0	10.9	1.29E-05		3/26/13 13:13
S37	7.127325	20.00	1.91E-04	247.0	11.0	1.41E-05		3/26/13 13:14
S38	7.177004	20.00	1.48E-04	247.0	10.9	1.10E-05		3/26/13 13:14
S39	7.17066	20.00	1.96E-04	247.0	10.9	1.46E-05		3/26/13 13:14

UV Dose Requirements

As of this paper, the optical power output of a single UV LED is very low compared to visible light LEDs. The LEDs selected for this research output approximately 0.00015 to 0.0002 W, as seen in Table 2 (SETi, 2013). Visible light LED packages that adequately replace conventional light systems are currently commercially available. A target dose of 40 mJ/cm² was selected by the other researchers; Major Tho Tran (2014) and Captain Kelsey Duckworth (2014). However, the practical power requirement is tenfold this value to generate hydroxyl radicals in the advanced oxidation process, which may be used to oxidize compounds. Several UV experiments dictate that a required dose will be at least 600 mJ/cm² and practical application should require more than 1000 mJ/cm² (Watts and Linden, 2008). Exposure time necessary to deliver an accumulated dose is dependent on flow and geometry. A lower power device requires longer exposure to the effluent to deliver the desired dose and, accordingly, a higher flow device requires more optical power. UV LED technology should improve with higher output LEDs as research progresses, so the flow rate or geometry of the vessel may change accordingly.

The lifespan and optical output of the LED are dependent on a series of relationships all linked by temperature. The dosage is calculated from the power output, which itself is approximated by the current input, as shown above in Table 2 (SETi, 2013). The driving current for the LED has a positive relationship with temperature (Perry, 2011). Unfortunately, the temperature of the LED has a negative relationship with optical power output, as shown in Figure 1, (SETi, 2012) and lifespan (Perry, 2011). This experiment has the potential to over drive the current in the LED which would produce a

large amount of heat. If the heat is not dissipated, then the experiment will not be as effective, nor will the LEDs last as long. It is imperative that the dosage is appropriate to reduce drive current to the required range.

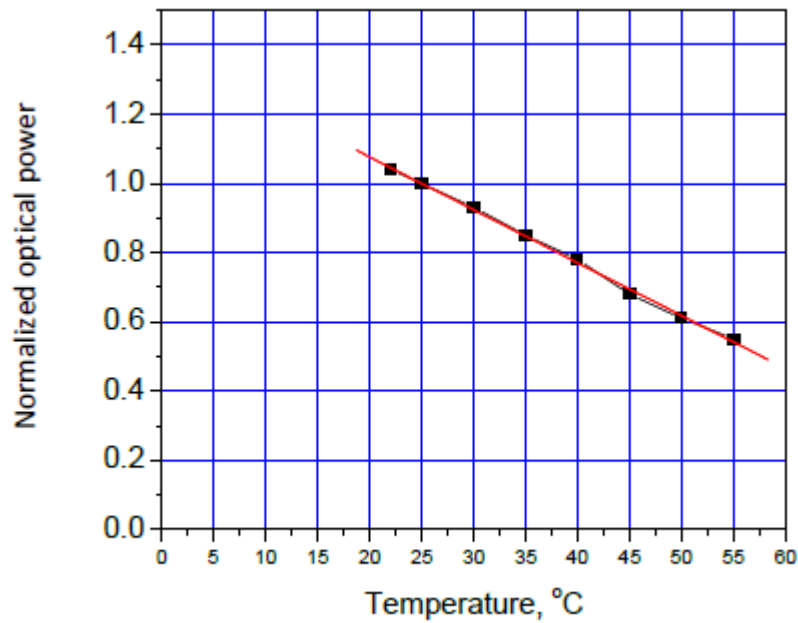


Figure 1. Optical power relationship with temperature (SETi, 2013)

Dispersion Pattern

There are distinctions in how UV energy is dispersed from LEDs compared to fluorescent bulbs. Fluorescent bulbs emit photons outward from the bulb in a radial pattern. In a research setting, Bolton et al (2003) utilized a “quasi-collimated beam apparatus” which manipulated the photons from a fluorescent bulb into a single direction, which made measuring the power output easier.

Photon emission from a fluorescent bulb and a quasi collimated beam apparatus is different from UV light propagation out of an LED, which can be approximated as a point source manipulated with a lens into several shapes, as shown in Figure 2. The LED emission incurs some optical loss through the lens. The lens with the least amount of loss is a planar, flat window which results in a pattern that is approximately a Lambertian Pattern. In a Lambertian Emission, the amount of radiation per square area is equal along the red outline in Figure 2. SETi provided a diagram of the typical output shape in air, seen in Figure 3, which approximately depicts a Lambertian Emission (SETi, 2012). Note that these measurements of the LED were into air, and output angles in water have yet to be defined in academia. Since the flat window allows the largest amount of energy to pass, and the experiments require the maximum output, this lens was selected for use in the initial system. The geometric output of the LEDs would have a considerable impact on the design of an effective reaction chamber

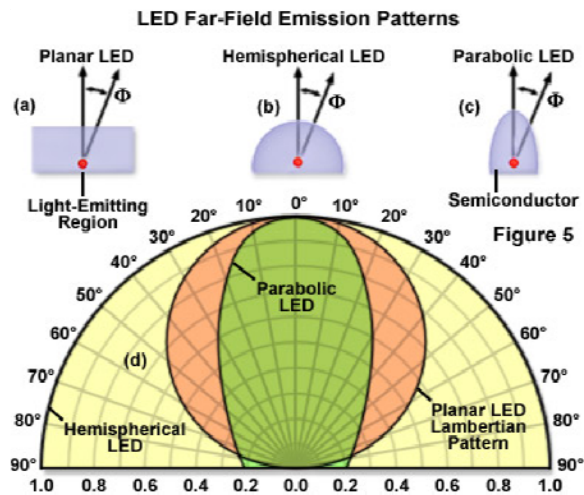


Figure 2. Variety of LED Lens emission geometry (Davidson, 2012)

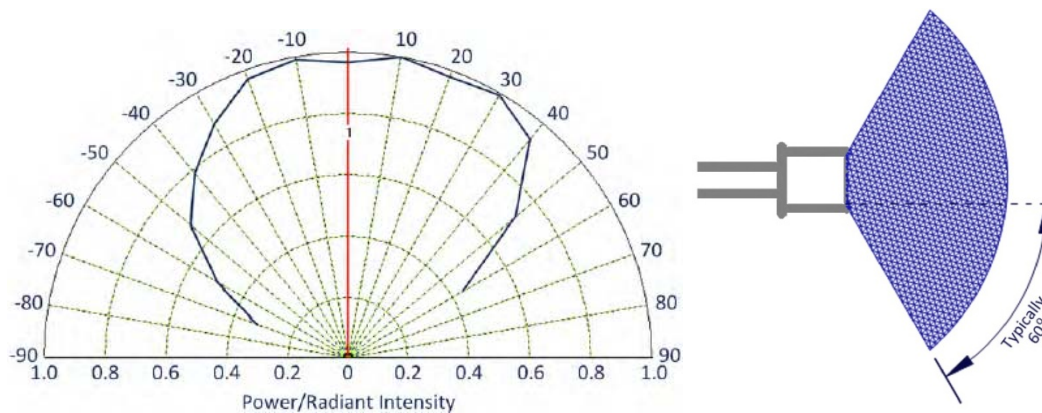


Figure 3. SETi UV TO39 Flat Window lens power intensity shape in air (S-ETi, 2012)

The UV LED's output angle can be predicted using Snell's Law. The manufacturer's advertised output angle of 60 degrees of UV energy in air, as shown in Figure 3, was further examined to understand the implications of the LED structure on the optical performance of LEDs in a water reactor. The structure of these devices is such that as UV energy is emitted from the substrate, it passes into nitrogen gas through the silica window into air. Since the index of refraction (n) of the nitrogen gas and air are both 1, the 60 degree output should also represent the initial output from the substrate inside the LED case. The angle internal to the silica window can be calculated using Snell's law, as shown in Equation 1. This law explains the relationship between the refractive index, n , and incident angle, θ , of each side of an optical interface, as shown in Figure 5.

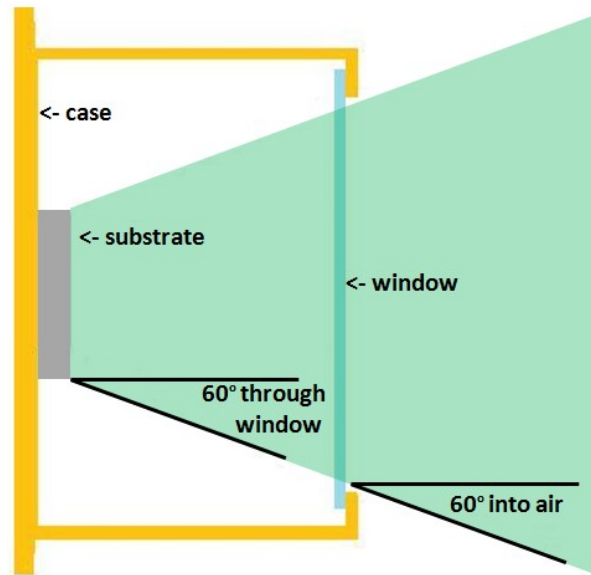


Figure 4. Light from LED substrate through silica window to air and water, figure not to scale

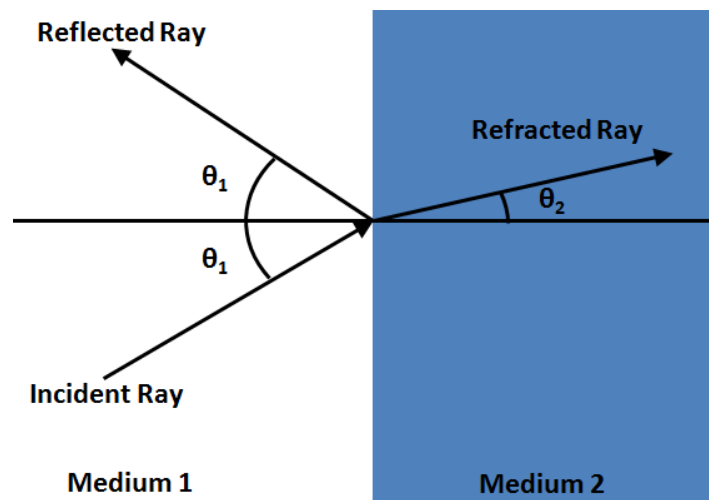


Figure 5. Diagram of Snell's Law as it applies to the UV LED window (Medium 1) and air or water (Medium 2)

$$n_1 \sin \theta_1 = n_2 \sin \theta_2$$

Equation 1. Snell's Law

Where:

n_1 = refractive index of medium 1

θ_1 = angle of the incident ray

n_2 = refractive index of medium 2

θ_2 = angle of the refracted ray

The UV LED output angle in water was predicted from the LED window's calculated internal angle. The initial angle from the substrate was assumed to be 60 degrees and applying the manufacturer's specification of $n=1.421$ for the silica window produced an angle of 37.6 degrees internal to the window. The angle into water can be calculated with Equation 1 utilizing the internal angle as side 1 and water as side 2. This analysis indicated that the predicted output angle into water would be approximately 39-40 degrees, since water has a refractive index between 1.3556 (for 270 nm wavelength light) and 1.3664 (for 240 nm wavelength light). For comparison, a more common refractive index for silica glass is $n=1.5$ (Refractive Index Database, 2013), which would then decrease the internal angle to 35.3 degrees. The output angle into water would not change due to a different window refractive index since the light enters and exits at the same angle. An effective vessel geometry should incorporate the LED output angle in water to reduce the incident angle with the vessel interior surface, thereby minimizing the reflection losses and reducing volumes where the radiation misses. This is discussed in-depth in the section labeled "LED Placement."

Optical Path Design

Optimizing the optical path of the UV light is a key characteristic of the reactor due to the low output of the UV LEDs. The type of loss discussed occurs when the light passes from one material to another and is reflected and refracted; inside the LED, at the LED-water interface and the water-vessel interfaces. The research did not focus on an in-depth investigation of the UV energy inside of the LED. The intent was not to redesign the interior of the LED itself, rather to provide a broad description of the optical path of the UV light before it enters the water. This path then could provide a better explanation of how the light will interact with the water, which was measured within this thesis.

Reflection and refraction inside the LED is critical to extract the most output from the LED. The UV LEDs emit photons from a substrate into a gas before exiting through a window, as shown in Figure 4 above. Snell's Law, Equation 1, describes the fact that the amount of light reflected is dependent on the refractive index, n , and angle of incidence, θ . As the incident angle increases, more light is reflected rather than passed into the second material. The first material change is from the substrate to the gas. There is little reflection and transmission data concerning the inside of the LED case. What is known for LEDs is that photons leave the LED substrate in all directions and impact the window at all angles, either directly, or after reflecting first off the interior of the LED case. Should the photon direction be controlled, the incidence angle should be kept as close to normal as possible to reduce reflection.

The incident angle is not controlled inside the SETi LEDs. The light passes from the substrate into nitrogen gas ($n=1$) to the silica window ($n=1.421$) (SETi, 2012). The interior metal surfaces of the SETi LED cases are plated to improve reflection of photons

not directly travelling from the substrate through the window. The amount of light reflected back into the LED case from the window is unknown as it is inside the LED. Limiting reflection at the window can be done utilizing a material with low refractive properties, such as quartz or fused silica (Newport, 2013), which SETi has done.

The total internal reflection of the silica lens was calculated since the light passed from the silica (material 1) into a less dense substance (material 2; air or water). The critical angle occurs when the output angle, θ_2 in Equation 1, reaches 90 degrees. Light incident beyond the critical angle would completely reflect back into material 1 instead of passing through. Figure 6 depicts the amount of internal reflection for photons traveling from a material with a refractive index of $n_1=1.5$ into another with $n_2=1$ for a given incidence angle. Utilizing the manufacturer specification for silica of $n_1=1.421$ (SETi, 2012), Equation 1 was solved for $\theta_2=90$ degrees to determine a critical internal angle, θ_1 , of 44.7 degrees. Using $n_1=1.5$ for the silica lens yielded 41.9 degrees. Therefore, photons incident to the boundary at more than 42-45 degrees will reflect back into the silica glass. The internal angles calculated in Table 3, 35.3-37.6 degrees, is less. So it can be assumed from these calculations that there was not significant light loss due to internal reflection in the silica-air interface.



Figure 6. Refraction angle dependence on angle of incidence due to internal reflection of a material with $n=1.5$ from which light propagates into a gas with $n=1$. Refraction angle greater than 90 degrees denotes the light is internally reflected inside material 1 versus passing into material 2.

The critical angle was calculated for the water reflective indexes, and the results are shown in Table 3. Since the reflective indexes of silica and water are more similar (water $n_2=1.3556$ for 270 nm wavelength light and water $n_2=1.3664$ for 240 nm wavelength light, Refractive Index Database, 2013), the critical angle was calculated to be much greater than the relationship with air. Therefore, less light was internally reflected compared to the silica-air interface.

Table 3. Internal angles of the fused silica-nitrogen gas interface and critical angles of internal reflection in silica-air and silica-water interface. Angles are in degrees.

	Internal Angle SiO ₂	Air n=1	H ₂ O n=1.3556	H ₂ O n=1.3664
SiO ₂ n=1.421	37.5	44.7	72.5	74.1
SiO ₂ n=1.5	35.3	41.9	64.7	65.6

The optical path at the UV LED-water interface should be kept simple to reduce optical loss. Ideally, the LED should be in direct contact with the water to avoid introducing further reflection. The LED should be sealed and pressurized to inhibit water infiltration, and the case material resistant to oxidation.

Reflecting the UV light inside the reactor vessel surface also improves efficiency of the system by reducing UV absorption. The reflectivity in air of potential materials has been studied in academic settings. This property was recorded as the real part of the refractive index, n , and imaginary, k . The total reflectivity can be calculated with Equation 2. A reflectivity of 1 describes perfect reflection, so the materials with higher values are desired.

$$\text{Reflectivity} = \frac{(n - 1)^2 + k^2}{(n + 1)^2 + k^2}$$

Equation 2. Reflectivity

Where:

n = real part of the refractive index

k = imaginary part of the refractive index

(Palik, 1978)

Table 4. Material reflectivity, calculated with Equation 2. (Palik, 1978; Palik, 1991)

	Wavelength (nm):			
Material:	240	260	270	Source:
Iron	0.4128			Palik, 1991
Copper	0.3778	0.3437	0.3347	Palik, 1978
Gold	0.3028	0.3558	0.3652	Palik, 1978
Osmium	0.5977	0.5939	0.5983	Palik, 1978
Tungsten	0.5406	0.4723	0.4551	Palik, 1978
Iridium	0.5467	0.5693	0.5668	Palik, 1978
Molybdenum	0.7042	0.6728	0.6582	Palik, 1978

Although this equation permits the reflectivity to be approximated, because this property was studied in an academic setting under near-ideal conditions, the practical application would not produce the same results. To achieve near-ideal performance, these materials were often produced as evaporated films in a vacuum to create the most pure

and smooth surface possible (Palik, 1978). The controlled settings were not available for practical application in this reactor. The exception to these impractical fabrication techniques is molybdenum, in which the data came from metal stock that was macro-etched, mechanically polished, electropolished, and annealed. Then “recleaned, electropolished, washed in acetone and then in ethyl alcohol, and transferred in air to the measuring apparatus” (Palik, 1978, p. 303). Unfortunately, it was not possible to procure molybdenum for this research as it would appear to have the highest reflectivity for use in a UV reactor. Stainless steel, which we approximate as Iron in Table 4, is readily available in many shapes, sizes, and high reflectivity forms. Shown in Figure 7, aluminum would have an even higher reflectivity, but “evaporated films show reflectances much higher than polished surfaces particularly in the ultraviolet” (Palik, 1978, p. 389). Figure 7 displays the enormous variance of reflectivity when encountering a less than perfect surface finish. The line shows the approximate wavelengths of interest. The dramatic reduction of reflectivity due to oxidation was a significant factor in determining reactor material. Oxidation was inevitable in this design, which was assumed to have a decreasing reflectivity as experimentation progressed. The variation of surface oxidation would decrease UV effectiveness in the vessel and increase error. Since it was assumed that stainless steel should maintain a stable reflectivity despite oxidation conditions, it should be considered for use in this reactor.

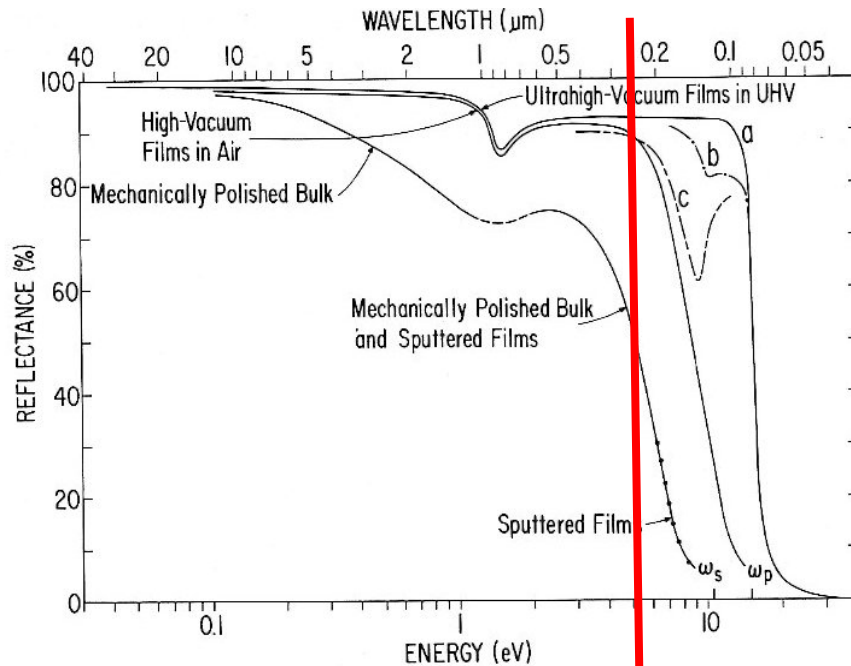


Fig. 12. The reflectance of metallic aluminum at room temperature. The uppermost curve gives the reflectance of opaque evaporated aluminum films prepared in ultrahigh vacuum. These films are presumed to be free of bulk and surface oxide contamination. The effect of light scattering and coupling to surface plasmons (at $\omega_s \approx 10.6$ eV) is illustrated by curves b and c. Curve b was obtained by Vehse *et al.* [90] for a film on a microscope slide cleaned by vapor decreasing and evaporated in a vacuum of $\sim 3 \times 10^{-8}$ torr; the “oxide-free” reflectance was obtained by extrapolation of the reflectance back to the time that the evaporation was completed. Curve c is for a uhv film with rms surface roughness σ of 18 Å, as reported by Endriz and Spicer [53]. The curve labeled high vacuum is an average for films evaporated in vacuum of the order of 10^{-5} torr. At this pressure surface and bulk oxidation occurs. The values reported for such films vary widely, especially in the ultraviolet, presumably because of surface roughness. The third curve is representative of mechanically polished samples, but the reported range of measurements is extremely large. Data for sputtered films are available from 380 nm well into the UV [44, 45]; curiously enough, they track the data for polished samples very closely.

Figure 7. Aluminum Reflectance and discussion. The line depicts the approximate position of the wavelengths of interest. (Palik, 1978, p. 389)

Vessel Material

Vessel material selection had to meet several specifications in addition to reflectivity. The experiments involved bacterial spore solutions and required sterilization. Therefore, the material and surface finish should be designed to endure several sessions

in an autoclave. The experiments were iterative in method, so the material must be cheap, easy to procure, and simple to machine. Lastly, the material had to tolerate multiple disassemblies and assemblies.

There were several surface considerations. A polished surface finish was imperative for two reasons. First, it would reflect UV energy as previously discussed. Second, a polished surface helps to prevent bacteria and chemicals from embedding in material pores and hampering sterilization and cleaning.

Surface interfaces in the design also impacted sterilization capability. Each edge or void would collect bacteria; a continuous containment vessel design, such as a sphere, would be ideal. A pipe design has fewer edge boundaries than a square or cube. Furthermore, straight connections from the flow through hoses to the vessel core would be preferred over hose adapters. The initial design utilized readily available silicone laboratory corks to seal the pipe adapters to the vessel. The corks allowed the hose adapters to be switched out as necessary. Future design should have a specific hose in mind and, therefore, the hose connector could be welded or brazed directly into the vessel core, thus removing as many interfaces as possible. Similarly, sealing adhesives would also provide microscopic voids in which bacteria would accumulate; limiting their use would be ideal. Sparingly applied silicone adhesive sealed the LEDs into the plate and the end plates onto the vessel.

The aforementioned criteria limited practical choices to aluminum and stainless steel. The selected vendor was the McMaster-Carr company, due to its close proximity, enabling expedited procurement. For the flat end plates, a mirror-finished plate of 5052 (corrosion resistant) aluminum and 316 stainless steel were readily available. One and

three-inch inner diameter, food-grade pipe was available in 316 stainless steel, with an internal surface finish of approximately 20 Ra (McMaster-Carr, 2012). To enhance the surface finish to approximately 10 Ra and remove surface discoloration and blemishes from welding, an electropolish session was performed on the final assembly (Electro-Polish, 2012).

LED Placement

The goal of LED placement is to ensure even UV distribution throughout the vessel. Even distribution ensures all the volume in the reactor is adequately irradiated and dead zones where no UV photons interact are reduced. Furthermore, an even distribution reduces areas of over-stimulation, where energy is wasted. Fluorescent bulbs emit in a radial pattern, making a pipe an easy design choice to contain the water. The quasi-collimated beam apparatus emits in one direction, which is ideal for a petri dish (Bolton, et al, 2003).

The LED emission is a circle on a two-dimensional plane facing the LED window, so a circle in that plane should produce an even distribution. This arrangement is considered for the initial vessel because it is the simplest configuration. A single LED could be mounted in the center of the circle, but when several LEDs are required for an adequate dosage, circle packing theory comes into play to ensure the most even distribution. Geometries based on 7 (Graham, 1968), 12 (Fodor, 2000), and 19 (Fodor, 1999) circles produce the most even arrangement, as shown in Figure 8. The seven circle geometry is the most beneficial considering the cost of each LED and experiment time based on dose calculated by the other researchers. Designs that follow the LED output

closer in three dimensions should be more effective. However, the output in water needs to be determined first.

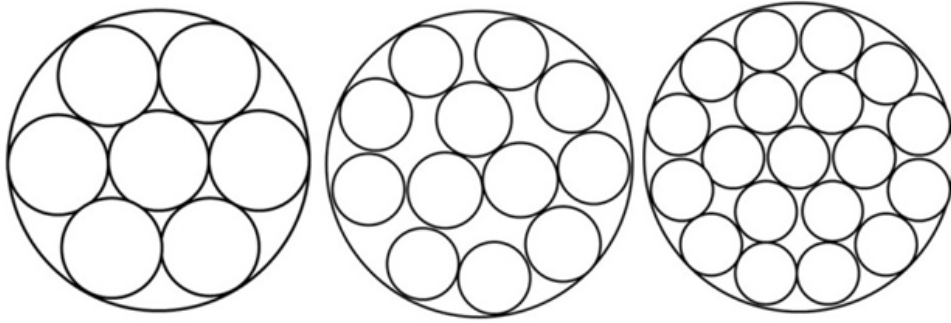


Figure 8. Optimized circle packing within a circle geometries: 7 (Graham, 1968), 12 (Fodor, 2000), and 19 (Fodor, 1999) circles

III. SYSTEM DESIGN, OPERATION, AND MODIFICATION

The geometry of the initial vessel design was carefully selected. A pipe design was selected for its simplicity, ease of construction, and speedy acquisition. The pipe design was easily cut into sections and welded onto the gasket plate, and the end plates were simply bolted onto the gasket plate, as shown in Figure 9. The arrangement of the LEDs on the end plates was easily, quickly, and cheaply modified. The first iteration had one LED centered on the pipe.

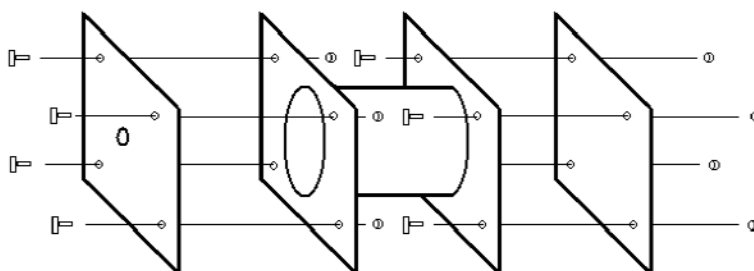


Figure 9. Initial apparatus exploded schematic without flow through pipes shown. Single LED hole shown in left plate.

Availability of several pipe diameters and end fittings was also attractive to the initial design. A three-inch pipe diameter was selected for the initial design, allowing for future arrangement opportunities. Other UV LED experiments utilized dishes as large as 14 cm in diameter with 250 mL of effluent. However, that size required radiation times of 30 minutes (Chevremonte et al, 2013). A three-inch pipe length was selected to create a simplistic three by three cube-dimensioned cylindrical vessel.

The problem of arranging the LEDs is more complex when considering a flow through system. This factor has been addressed with the previously depicted fluorescent

bulb systems, which use pipes as the reaction vessel. The designs demonstrated by other UV LED research, Bolton (2003) and Chevrement (2006), were not flow-through.

The initial specifications require a simple flow-through design, with a volume flow rate of less than 10 mL/minute. One-inch diameter pipes were selected as connections which utilize off-the-shelf laboratory stoppers and provide enough cross section to change connections should it be required later. They were staggered on opposite sides of the pipe to facilitate mixing inside the vessel, as shown in Figure 10. In-depth fluid dynamic evaluation should be completed for future designs. The assembly would be welded together.



Figure 10. Completed initial reaction vessel; three inch diameter and three inch length main pipe, one inch diameter flow through pipes all made of sanitary, food-grade finish 316 stainless steel pipe, final polishing via electro-polish process.

LED Control Components

The control components had to fulfill two requirements. First, the electronics had to run the LEDs at the specified amperage and pulse drive for the experiments. Second, in the multiple-LED system, it was necessary for these components to compensate for the gross electrical variability between the LEDs, as shown in Table 2, to ensure each LED emits a predictable amount of power. This variability also was attributed to the inconsistent effective resistance of the LEDs, which had to be resolved.

The fundamental LED control system for amperage and pulse drive was already developed by the research team. A computer software program controlled the voltage and was able to collect analog feedback data to control the system through a USB board, as shown in Figure 11. The USB board output a single analog voltage (0-10V) to the electronics board to control all the LEDs. The USB board had the capability to collect data from the electronics board, which could then be used to protect the LEDs from over- or under- driving.



Figure 11. USB board made by Measurement Computing

The USB board connected to the LED drive board which contained the power supply and electronic components which supplied electricity to the LEDs, as shown in Figure 12. The initial power supply was a simple transformer-based ± 24 volt system capable of 0.6 amps. Twenty four volts gave adequate flexibility for later modification and 0.6 amps is adequate for steady state operation since each LED would use 20 mA. Switching Mode Power Supplies capable of 4 amps were later used in anticipation of using more current in pulsed mode. Connections to the electronics board were via 1/8-inch pins, which enabled a quick, but secure connection. The heart of the LED drive board was a following operational amplifier (OPAMP) which provided a voltage output that mirrored the input voltage. The input voltage initially operated off of the USB output voltage. The following OPAMP isolated the USB board output voltage from the LED drive power supply, thus eliminating large amounts of current to pass back to the USB board. The USB board only had to supply minimal voltage and amperage, while the electronics board supplied the amperage to the LEDs. The LED drive board was mirrored with 12 LED connections, with a voltage input for each side, labeled Input A and Input B. The intent was to enable the use of the maximum number of LEDs that the initial power supply amperage could handle, 24 total at 20 mA. Although each experiment ultimately only used up to seven LEDs at one time, the mirrored configuration was later found invaluable because it allowed multiple modifications to the control system without significantly changing the electronics board.

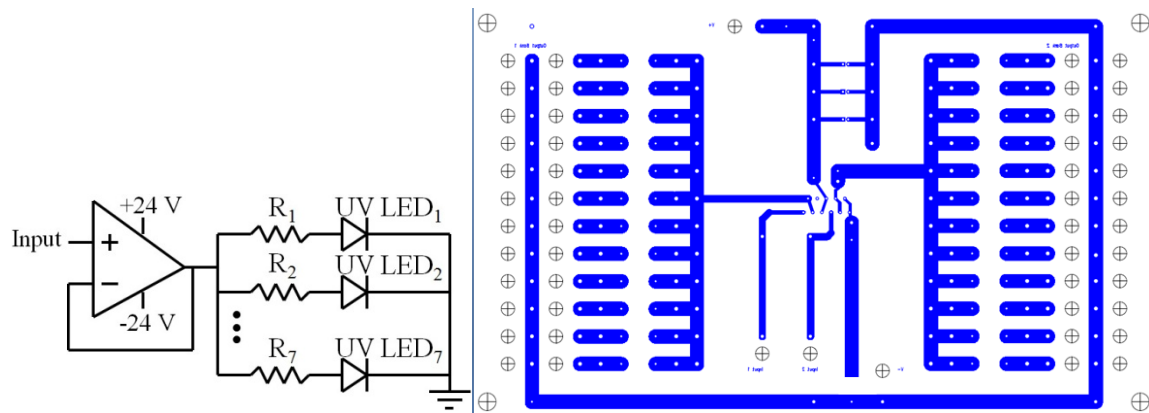


Figure 12. LED Drive Board schematic and trace diagrams

The system operation was kept simple. The USB board was attached to the common ground for all measurements and output. The USB output voltage attached to either the a or b input voltage pin hole on the LED drive board. In the initial design, the voltage ran directly to the following OPAMP. The USB board was limited to 10 volts, which was not high enough for some experiments. A multiplying OPAMP was later inserted between the USB output and following OPAMP input, enabling 24 volts, which was the maximum the power supply allowed. The following OPAMP opened the isolated circuit to the voltage set by the input. Amperage then flowed from the power supply through the following OPAMP to the individual LED branches. Each branch had a resistor and pin holes for electrical measurement in series with individual LEDs.

The resistors were initially selected to provide protection to the LED in the case of overloading by amperage or voltage, calculated by Ohm's Law in Equation 3. The 240 nm wavelength LEDs required different resistance than the others since the turn-on voltage was 7 volts versus 5 volts for the 260, 265, and 270 nm wavelength LEDs. The resistance was later changed to 50 Ohm to easily verify 20 mA current with a volt meter,

which should read 1 volt per Equation 3. Next in each branch were pins for measuring the current or voltage. The amperage then left the board pin on an 18 gauge wire which was soldered onto the LED lead. The static resistor allowed measurement of the amperage flow, calculated with Equation 3 and the measured voltage across the resistor.

$$V = I R$$

Equation 3. Ohm's Law

Where:

V = volts

I = amperage

R = resistance

Construction and Operation

The reactor design and construction was iterative as researchers progressed. The core pipe assembly was kept very simple, which gave the AFIT machine shop flexibility to fabricate the part quickly. The vessel core was polished with an air grinder to remove welding marks before being sent to Electropolish in Dayton, OH to improve the overall surface finish (Electropolish, 2012). The design of the initial reactor LED plates and subsequent heat sinks were completed on a computer aided design program, which enabled precise changes to the design and allowed the machine shop to cut the plates quickly on a water jet cutter. Plates of steel and aluminum were cut. The plates were designed such that the LED would fit through, directly touching the water. The LED was sealed with silicone caulk to the plate and was soldered to the wires for durability. A back plate or, later, heat sink secured the LED to the plate. The other researchers

acquired their own pumps, hoses, and experimental measuring equipment for their specific research. Major Tho Tran initially used a flow through design, but it was later impractical due to the use of an orbital shaker, shown in Figure 13 (Tran, 2014). Major Tran's reactor vessel flow-through pipes were sealed to create a batch-type experiment design. Captain Kelsey Duckworth used the seven LED plate, flow-through design system pumping to a UV Vis measurement device, as seen in Figure 14 (Duckworth, 2014).

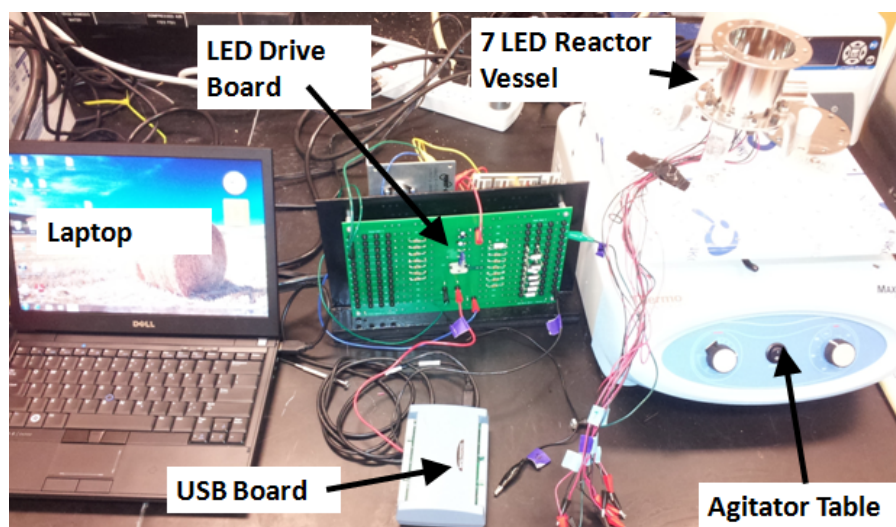


Figure 13. LED system set up as a batch design with flow through pipes sealed and mounted on an orbital shaker (Tran, 2014)

The control system was a joint effort. The software and USB board were selected by the research advisors. The task of operating the control software was given to Captain Bates. Captain Bates used the LED drive board only, since he used the Labsphere apparatus, shown in Figure 15, to measure the LED output (Bates, 2014). The LED drive board was designed by the faculty and assembled as part of this thesis.

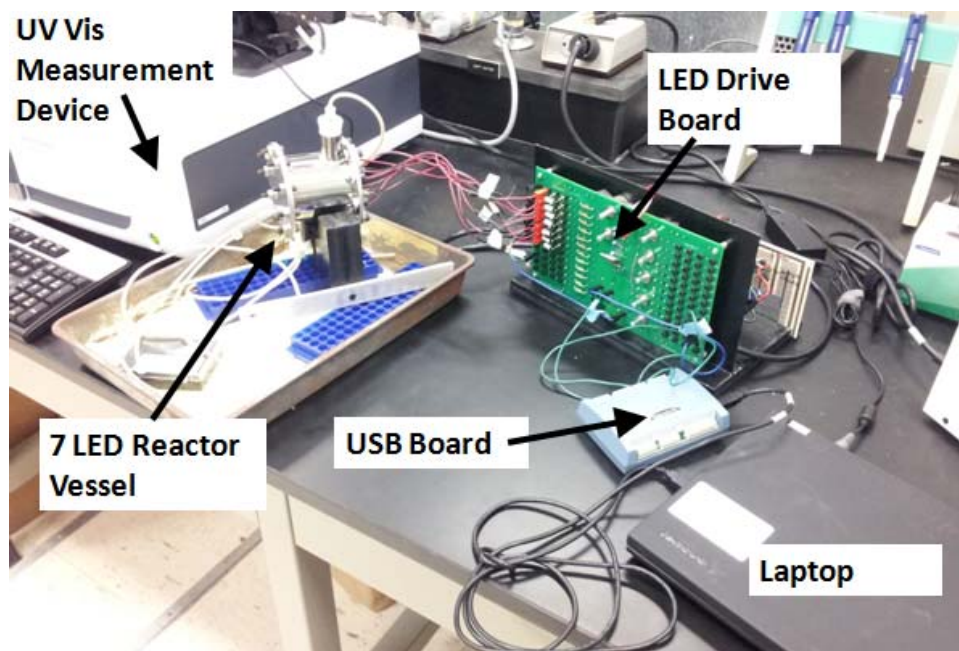


Figure 14. Flow through reactor system with silicone hose connecting to a UV Vis measurement device (Duckworth, 2014)

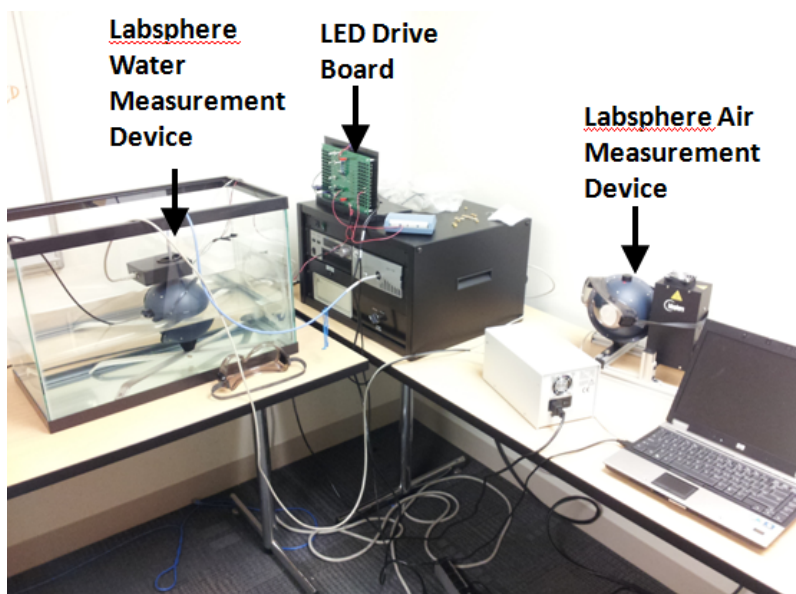


Figure 15. Captain Christopher Bates' LED measurement system utilizing the LED drive board with Labsphere air and water measurement vessels (Bates, 2014)

LED and LED Plate Modifications

There were several changes to the reactor system as research progressed. The plates were first to be modified. The initial experiments quickly revealed that a single LED produced an inadequate dose, and the other researchers found that seven was more acceptable for their experiment designs; both versions are shown in Figure 16.

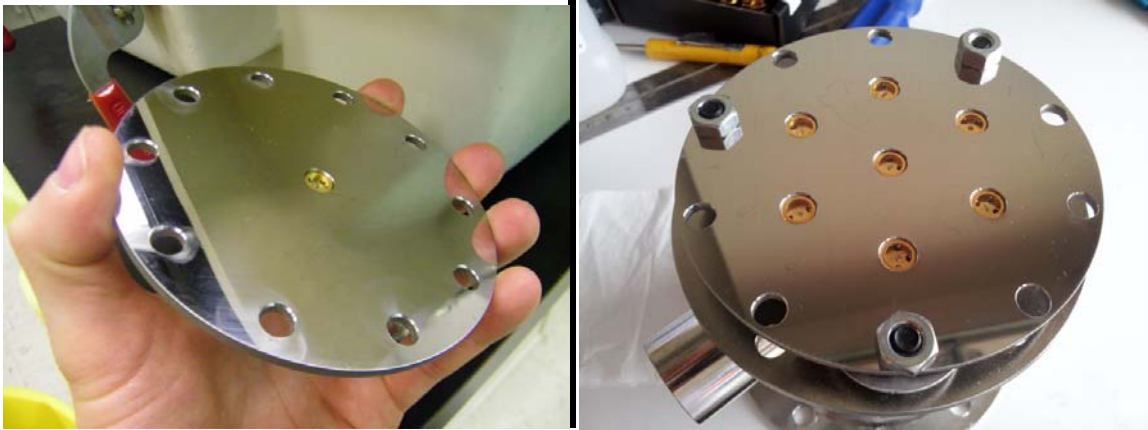


Figure 16. Single LED plate and seven LED plate

The LED was in contact with water, so a proper seal was critical. A silicone gasket sheet was initially used. The gasket allowed quick assembly, but it was too fragile. Liquid silicone sealant was used for the rest of the experiments. Unfortunately, it required curing time. Ideally, a robust gasket sheet should be used to enable the LEDs to be replaced and used immediately. One LED experienced water infiltration inside the case after being overdriven for 24 hours. The probable cause is that the silica window has a very small heat expansion coefficient compared with the metal case. Also, the plating on several LEDs was removed by the advanced oxidation process and the case material rusted. That issue was not resolved.

A heat sink made of aluminum was created to handle the anticipated heat load and secure the LEDs to the plate in the new geometry, as shown in Figure 17. Thermal paste was used to enhance heat transfer from the LED to the heat sink. Maintenance on the system was constant throughout the research time. The most reoccurring task was to replace LEDs that were not performing properly. This process used a lot of time as it required precise application of silicone and solder.



Figure 17. Aluminum heat sink bracket

Reactor Vessel Modifications

The reactor vessel core was only modified once. Major Tho Tran's experiment utilized a bacterial spore solution that inadvertently settled in the vessel. Brackets were made to mount the vessel on an orbital shaker. The experiment was no longer flow-through, so the pipes were sealed with silicone and aluminum foil to make a more continuous vessel, shown in Figure 18. The wires from the LEDs were attached to the shaker to reduce stress on the LED pins (Tran, 2014).

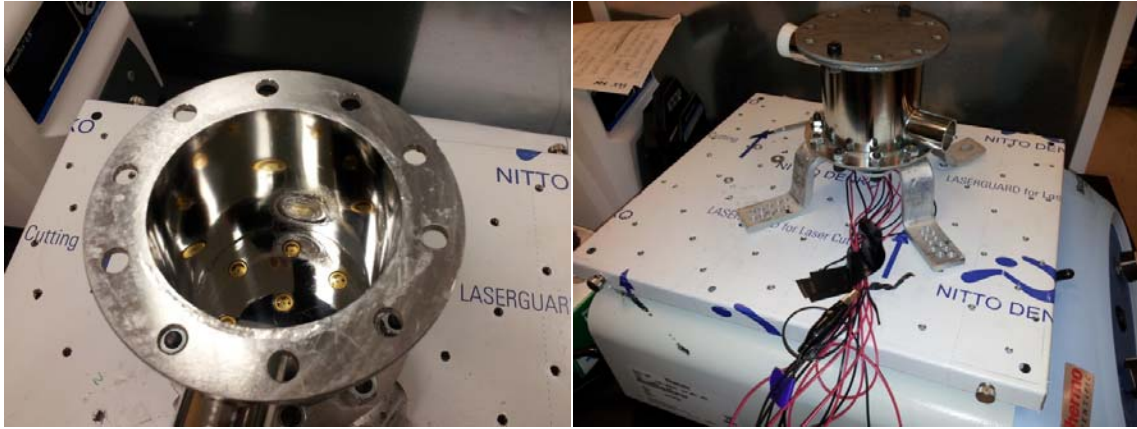


Figure 18. Reactor vessel with flow through pipe sealed

LED Drive Board Modifications

The LED drive board was modified with resistors used for over-voltage safety, voltage compensation, measuring amperage, and controlling amperage. An additional OPAMP board was also added to increase input voltage. The initial safety resistors were required due to accidental over-volting. This occurred when the board input voltage was not connected to a ground or USB board and the OPAMP would output a floating voltage. The resulting voltage spike would exceed the LED specifications for voltage and amperage.

The USB board was limited to 10 volts, which was inadequate for driving some experiments. An amplifier board was assembled and installed on the back side of the LED drive board, as seen in Figure 19. The amplifier board connected directly to the LED drive board, using the same power supply and connected directly into the existing board circuit. The input signal from the USB board was intercepted from the input pin. The selected resistors, $R_F=470$ and $R_I=330$, multiplied the input voltage by 2.4, per Equation 4. The result expanded the input voltage range from 10 volts to the power

supply maximum of 24 volts. The signal was soldered back onto the input trace to the LED drive board. The amplifier board was installed such that the connections on the board would not change.

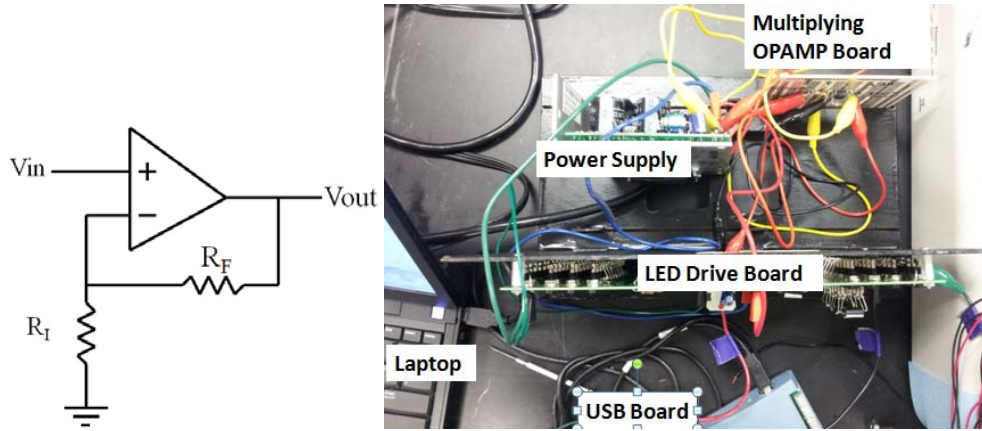


Figure 19. Input voltage multiplying OPAMP schematic and diagram

$$\frac{V_{OUT}}{V_{IN}} = \frac{R_F}{R_I} + 1$$

Equation 4. Amplification Ratio

Where:

V_{IN} = input voltage

V_{OUT} = output voltage

R_F = resistor 1

R_I = resistor 2

The variability of each LED presented a unique problem. The primary issue was that for a given voltage, each LED permitted a unique amount of amperage. Amperage translated to an approximate optical power specification supplied by SETi. The

researchers would design their dose around the optical power specification. The company measured the LED optical power at 20 mA (SETi, 2013). Therefore, it was the goal of the researchers to maintain 20 mA throughout the experiments to ensure the optical output from the LEDs was approximately constant. The researchers created two approaches to equalize the amperage to each LED.

The first direction was to install variable resistors in line with each LED branch and vary the resistance until the amperage was 20 mA, as shown in Figure 20. The variable resistors were connected to right side of the board. This approach became tiring and error prone since the electrical characteristics of each LED changed as the LEDs warmed up and changed differently as they aged. The researcher was required to equalize the system before each run. The variable resistors were not measured at each turn and introduced immeasurable error into the system. This research found that the LEDs would require a lower voltage as the LED aged to maintain the constant current. Without a compensating feedback loop, the longer experiments were prone to over-radiating since they allowed more amperage through as time progressed. This error would make it seem that the system was more effective.

Another approach found later was a constant-current resistor, which is also shown in Figure 20. The resistors are connected to the left side of the board, in series with the measuring resistors. The constant current resistors are off-the-shelf components specifically designed to work with LEDs which limit the maximum current flow. The new resistor maintained an even voltage and amperage to the LED despite an increasing input voltage. The specific model was a 20 mA LUXDrive produced by DynaOhm (Superbrightleds, 2014). This solution also worked with a square wave pulsed drive. The

addition of the multiplying OPAMP on the input voltage was critical when applying these components since the constant current resistor used at least 5 volts. This combined with the measuring resistor (1 volt) and LED (5-7 volts) far surpassed the 10 volt limit of the USB board output.

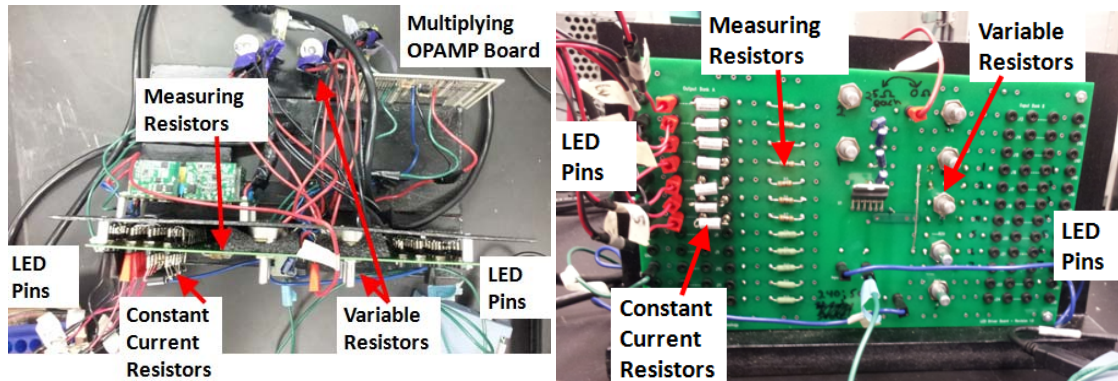


Figure 20. Variable resistors and multiplying OPAMP board added to the original LED drive board

Operational checklists should be used. In general, checklists improve experiment result precision and repeatability. They also protect the LED from overvoltage or over amperage. The primary cause of exceeding the LED electrical specifications was due to input float. This occurs when the LED drive board input was not connected to the ground or USB board and the resulting voltage in the system varies uncontrollably. The solution was to have the researcher double check all connections and on the computer software set the voltage to 0 before turning off the equipment.

IV. CHARACTERIZATION OF LED OUTPUT IN WATER

Introduction

Although Snell's Law was applied to determine the output angle of the LEDs in water based upon specifications provided by SETi corporation, this attribute of the LEDs is critical to future reactor design. Therefore, an experiment was designed and conducted to understand the angular output of UV LEDs in air and water.

Methodology

Measurement of the UV LED output in three dimensions (3D) in water was accomplished in the following manner. A quantum dot sheet was obtained and mounted perpendicularly to the LED face on the water side of the tank, as shown in Figure 21. A quantum dot sheet is a plastic substrate coated with quantum dots. Quantum dots absorb passing photons and emit them at a longer wavelength (NANACO, 2014). Therefore, the UV light became visible and a digital camera was able to capture the emission pattern. This created an effective cross-section imaging tool. A transparency sheet with 0.25-inch grid squares printed on it was sandwiched between the plastic and glass to reduce optical effects through the glass. The transparency sheet was ultimately printed on a laser jet printer to prevent the ink from dissolving.

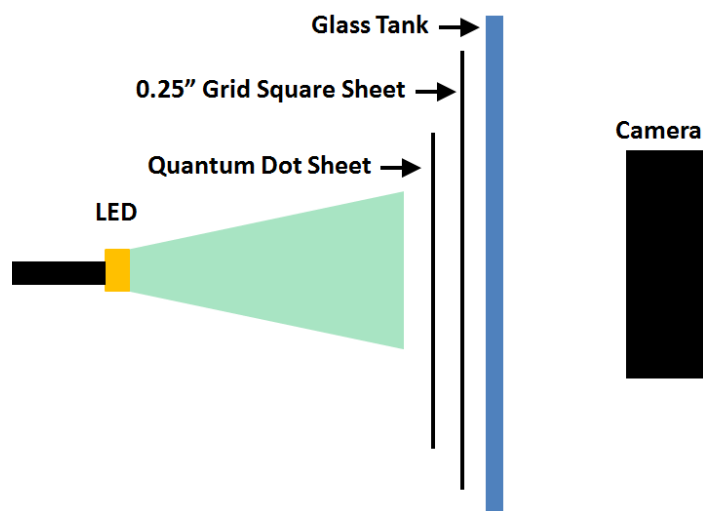


Figure 21. Diagram of the plastic sheet mounted on the water side of the tank

The subject LED was mounted in the water on a moving assembly such that it traveled on the axis facing the plastic sheet, shown in Figure 22. The LED was sealed onto a small plastic insert with silicone, simultaneously waterproofing the electrical connections. One LED of each wavelength (240, 260, 270 nm) was attached to its own insert. The inserts slide onto the arm for quick disassembly. A ruler was attached to the tank beside the LED assembly to track travel distance. The LED was driven with a digital power supply to provide precise control of the input current. During measurements, the room was darkened since the quantum dot sheet reacted with all wavelengths of light.

Measurements were conducted using the following steps:

1. Assemble system as described, with the LED moving assembly at position 0 on the ruler and the LED against the quantum dot sheet.
2. Turn on the power supply and adjust the voltage until the desired amperage is achieved. Allow the amperage to stabilize. Adjust the voltage as the experiment progresses to maintain steady amperage.
3. Adjust camera so it is properly focused and lock the focus.
4. Darken room.
5. Take image at point 0, move assembly 1 mm, take image, repeat until 10 mm. Then take an image every 2 mm until 30 mm. Any light used to aid moving the assembly should be turned off while taking the image.

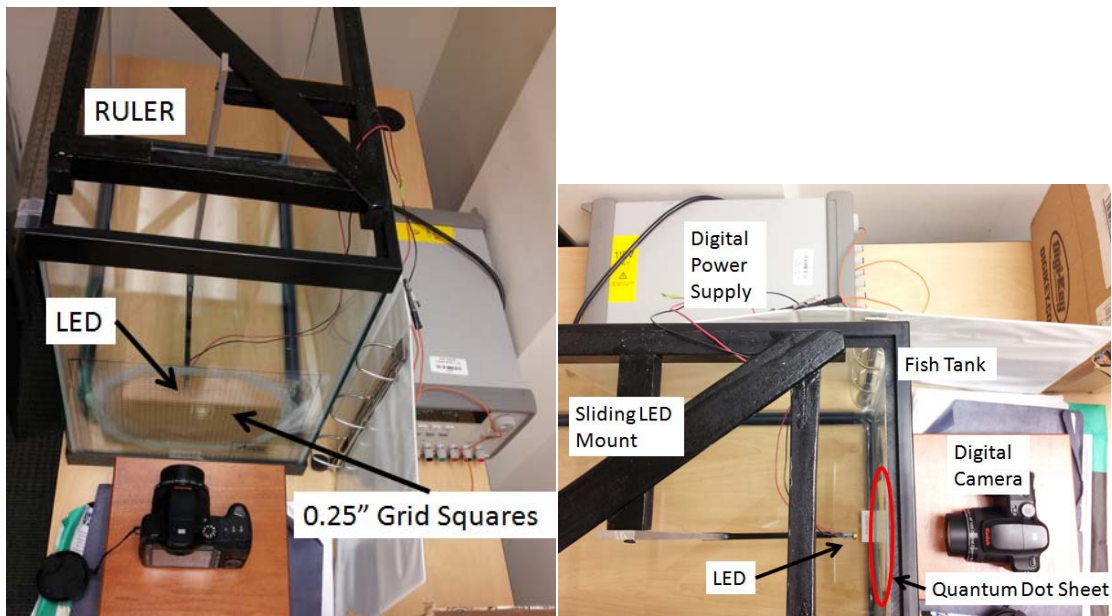


Figure 22. Diagram of the LED geometry output measuring device

Air Data Analysis

The measurements in air were analyzed first. The angle was calculated by measuring the diameter of the output circle, subtracting the LED lens diameter, and compensating for the distance from the LED. Figure 23 shows an example of the 0.25" grid (with 0.125" underlay grid) output in white light. The right side of Figure 23 gives an example of the output that is measured.

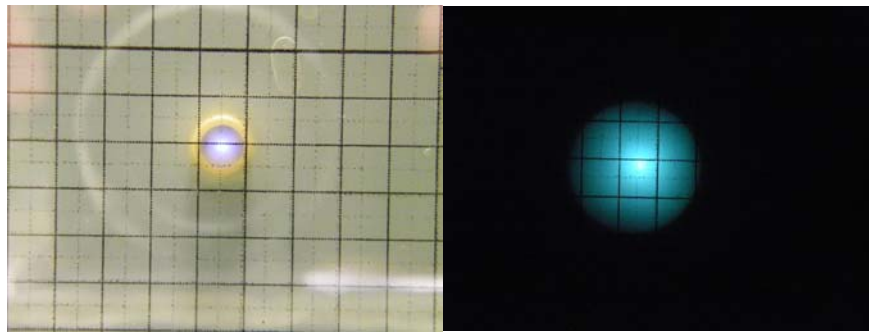


Figure 23. LED water output through quantum dot sheet in white light (left) and dark room conditions

The diameter of the light-dark boundary was measured using the grid squares to extrapolate the actual distance. The average of three measurements around the circle was recorded in a spreadsheet and plotted to produce a linear equation. The slope of the linear equation was compared against the slope of the diameter calculated with Equation 5 from a specific angle, as shown in Figure 24. The angle that produced the closest slope was presumed to be the approximate angle of the LED output. The air measurement results are tabulated in Table 5. The full set of plots are in the Appendix.

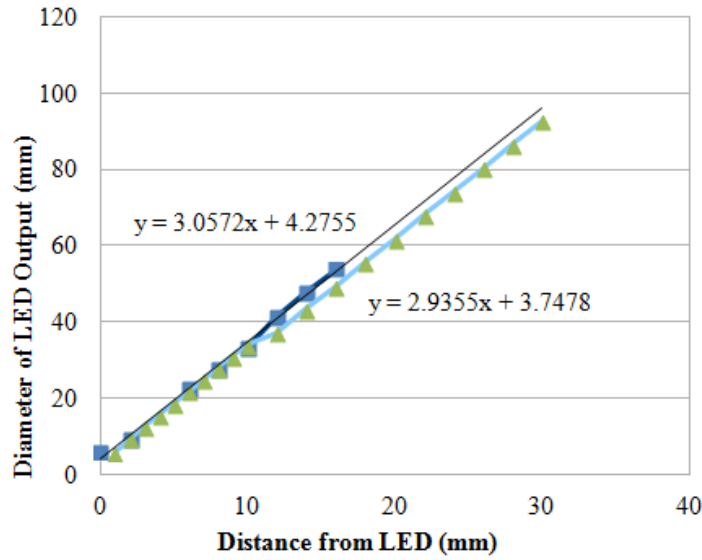


Figure 24. Example output comparison between measured (squares) and predicted angle (triangles)

$$\text{Predicted Diameter} = 6.48 + 2(d)\tan(\theta)$$

Equation 5. Predicted Diameter of Output

Where:

6.48 mm is the diameter of the LED window

d = distance between the LED and the measuring sheets

θ = predicted angle

The first air measurement attempt produced inaccurate data as an analog power supply was originally applied which did not produce stable amperage. Therefore, the experiment was repeated using a digital power supply. Furthermore, the initial measurements at 20 mA produced dim pictures, so the second run was accomplished at both 20 mA and 30 mA for all three LED wavelengths. The second air measurement

results were used. The weak output at 20 mA resulted in ambiguous data for the 260 and 270 nm wavelength LEDs. The 240 nm wavelength LED produced no discernible data at 20 mA.

Table 5. Measured LED output angles (degrees) in air and water output prediction

Air:	Output Angle:	Angle Internal to SiO₂:	Predicted Water Output Angle:
260 nm at 20 mA	63-65	38.8-39.6	41.1-42.0
260 nm at 30 mA	59	39.6	39.2
270 nm at 20 mA	64-65	39.2-39.6	41.5-42.0
270 nm at 30 mA	58	36.6	38.7
240 nm at 30 mA	58	36.6	38.4
240 nm at 40 mA	63	38.8	42.0

The data was used to compare the SETi specifications and calculate predictions for the water measurement. As previously discussed, the SETi diagrams show the LED emitting at approximately a 60 degree angle, as shown in Figure 3. The data collected in the air measurements provided approximately the same result, as shown in Table 5. To predict the output in water, Snell's Law, Equation 1, is first used to determine the light angle, θ_1 , internal to the fused silica (SiO₂) LED window ($n_1=1.421$) (SETi, 2012) from the air measurement angle, θ_2 , at the LED-air interface. The calculated internal angle is then used to predict the output in water ($n_2=1.3556$ for 260 and 270 nm and $n_2=1.3664$ for 240 nm) (Refractive Index Database, 2013) at the LED-water interface.

Amperage became an unpredictable variable on output angle. The 260 and 270 nm wavelength LEDs both measured smaller angles by 5 degrees, but the 240 nm wavelength produced the opposite. One possible reason might have been that the camera was not collecting the full output in the air measurements. This is critical since the outside diameter, the dimmest portion, was the measurement. It could be possible that the center portion of the picture was too bright and the digital camera was not allowing itself to over-expose the center to adequately image the true outside edge of the light. Additionally, it might be possible that the converted photons passing through the quantum dot sheet did not get collected by the digital camera when they are so dim. If this were true, then another UV detector needs to be used, such as a fluorescent dye.

Water Measurement Analysis

The water measurements were conducted just like the air measurements with the exception of the tank being filled with deionized water. In the first attempt, the grid square ink dissolved in water since it was printed on a standard ink jet printer. Despite the hurdle, the measurements were accurate. A second attempt, with the grid squares printed with a laser printer, confirmed the accuracy. The 260 and 270 nm wavelength LED output tabulated in Table 6 used the second attempt measurements and the 240 nm wavelength LED output was taken from the first attempt.

There was a constant difference between the predicted and measured water angle values, as shown in Table 6. There are two reasons that could explain the discrepancy, and they both point to problems with the air measurements since the water measurements show a very definitive border between light and dark as compared to the air

measurements, as seen in Figure 25. Together, these two reasons suggest that the water measurements may be more correct than the air measurements. The reason explanation is uncorrected error when measuring the diameter, as discussed in the previous section.

Table 6. Measured LED output angles (degrees) in water and difference with water output prediction

Water:	Measured Output Angle:	Predicted Water Output Angle:	Difference:
260 nm at 20 mA	43	41.1-42.0	1 to 2
260 nm at 30 mA	43.6	39.2	4
270 nm at 20 mA	46	41.5-42.0	3.5-4
270 nm at 30 mA	45.5	38.7	6.8
240 nm at 30 mA	46.5	38.4	8

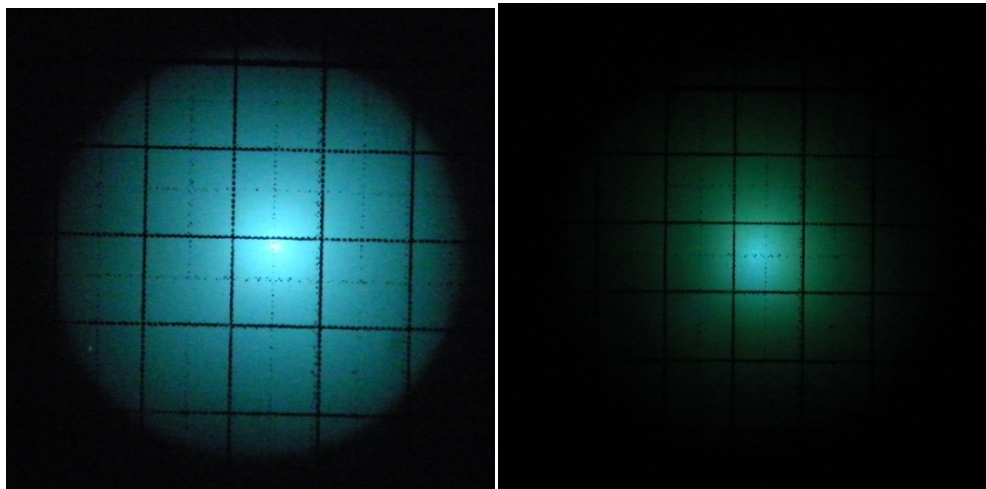


Figure 25. Example water measurement showing distinct border between light and dark (left) and air measurement (right)

The second reason is that the UV light incident angle surpassed the critical angle of the LED window. Using Equation 1 to back-calculate the internal angle of the silica window ($n=1.421$) and assuming the water output of 45 degrees is accurate, the result is approximately 42.5 degrees. This also assumes that the refractive indices previously used are the same. That internal angle would result in an air output closer to 74 degrees. Snell's Law may identify the angle, but the magnitude of output would be hampered by the critical angle. Table 3 shows that the critical angle for light passing from the silica window ($n_1=1.421$) into air ($n_2=1$) was 44.7 degrees, to which 42.5 degrees is very near. Figure 6 shows the exponential increase in reflection as the incident angle nears the critical angle. The critical angle is worse if the more common refractive index of the silica window, $n=1.5$, is used. It returns a critical angle of 41.9 (Table 3). If this were true, then the air measurement does not measure the total output as the outer-most angled light was most likely reflected back inside the window and that Snell's Law does not accurately predict this relationship perhaps due to the presence of internal reflections in the LED window.

V. CONCLUSION

Summary

This thesis research ventured to advance the application of UV LED technology to UV water treatment. The long-term goal is to replace current equipment that uses UV fluorescent bulbs that are electrically inefficient, have a short lifespan, and are fragile. The problem is that the fluorescent bulbs emit photons in a much different manner than LEDs and the reactor vessel and control systems should be studied to optimize effectiveness.

Two questions were answered in this thesis. First, what characteristics should be considered at the LED-water interface and water-reactor vessel interface when designing a reactor? Seven characteristics were identified in the literature review and practical application: LED wavelength, UV dose requirements, dispersion geometry, LED placement, optical path, vessel material, and LED control components. Each can be optimized for application to water treatment. Secondly, what is the UV energy output geometry in water and how can the reactor geometry be optimized accordingly? The UV LED output measurement in water determined that a TO39 case, flat window LED produces approximately a 45 degree angle in water. The angle is not precise due to the variability between individual UV LEDs and different specified wavelengths. A different lens or LED configuration will produce a different angle. Most importantly, a UV water treatment system was created for use by other researchers.

Preliminary research was conducted to create an initial experimental reactor. This vessel was then operated and modified for other simultaneous research efforts, which involved treating water solutions of bacterial spores for disinfection studies (Tran, 2014)

and methylene blue to measure oxidation (Duckworth 2014). One further thesis created a computer model which calculated a three-dimensional diagram of the LED normalized power output inside the reactor vessel (Richwine, 2014). This research then measured the LED angular output in water. Along with further in-depth investigations, the cumulative research identified several system characteristics and vessel geometries which may be more effective at treating water with UV LEDs.

The early investigation found that the UV LED-vessel interface should maintain the highest optical efficiency to compensate for the relatively weak output of this new technology. This started with the LED lens, where the most unrestricted geometry should be selected. In this case, a flat or planar window produced the least optical loss. In air, the geometric dispersion of the UV radiation for this lens can be characterized as a Lambertian Emission. The shape of the output in water was defined after the initial reactor was constructed, and material procurement drove the decision for the initial reactor geometry. Future reactor geometries should take into consideration the type of lens and subsequent output in water.

The initial UV LED vessel balanced optical efficiency with constructability and practical flexibility in experimentation. The reactor interior surface should be as reflective as practical to limit UV absorption. This was balanced with other material requirements of the reactor, such as sterilization capability, oxidation resistance, and ease of procurement and construction. Readily available, polished 316 stainless steel food-grade pipes, later electro-polished, and mirror finished plates were selected to create the vessel. The three-inch diameter pipe was capped at both ends with removable, mirror-finished plates to which the LEDs were mounted. One-inch polished pipes were attached

in a staggered configuration to the side of the three-inch pipe. The pipe size allowed standard corks to be used and the corks allowed flexibility in the manner that the flow-through hoses or pipes were adapted to the vessel.

The reactor system was modified as research matured. The initial experiments proved that more power was required than a single LED could output for practical experiment design, and the LED plates were modified to mount a total of seven LEDs. Next, the turn-on voltage for the 240 nm wavelength LEDs was higher than anticipated and, together with the safety resistor, exceeded the USB board output voltage. A multiplying OPAMP was installed in-line with the input trace, thereby allowing the input voltage to increase to the maximum allowed by the power supply. When the system expanded to seven LED plates, variability between the individual LEDs output needed to be leveled. First, variable resistors were installed in-line with each LED, but that was approach proved inaccurate. The second approach was to replace the variable resistors with constant current resistors, which limited amperage to a predetermined amount. These modifications were sufficient for the advanced oxidation process experiments, but the bacterial spore solution required one more modification. The bacterial spores in the solution settled to the bottom of the vessel and into the areas between the LED output cones. The flow-through design was replaced with a batch-type system so that the assembly could be mounted on an orbital shaker. The shaker created sufficient stirring so that the bacteria did not settle. These modifications allowed other researchers to successfully meet their objectives.

The measurement portion of this thesis endeavored to determine the UV LED output angle in water. The air measurements successfully replicated the 60 degree output

angle specified by the manufacturer. There were, however, caveats when translating the output angle to water. First, the input amperage did not have a consistent relationship with the output angle. Two different amperage inputs, 20 and 30 mA, were used to compensate for the dim images in the air measurements. Increasing the amperage actually decreased the output angle by 5 degrees in the 260 and 270 wavelength LEDs, but the opposite effect was observed in the 240 nm wavelength LED, as shown in Table 5. Secondly, the output images in air were very dim where the diameter was measured. It may be possible that the quantum dot sheet did not allow the weak, outer-edge photons to pass because they lacked the necessary energy to be converted to a longer wavelength. Another possibility is that the camera was unable to capture the photons, another symptom of weak light, especially considering that the camera compensated for the very bright center of the image. Lastly, it was calculated that the light was internally reflected inside the UV LED window when shining into air. This was due to the incident angle internal to the lens nearing or surpassing the critical angle for the LED window-air relationship. As a result of these events, the air data consistently predicted a lower output angle in water than what was measured. The flat window UV LED's output angle was measured as 43-46 degrees in water, which was 1-8 degrees greater than predicted.

Future Design Considerations

There are several concepts that are recommended for further research and potential implementation into design. They fall into three categories: LED design, vessel design, and control system. There are some basic changes to the LED design that may

increase output. Starting with the substrate itself, visible light LEDs have improved performance by simply changing the position of the substrate. One company has produced the LED substrate on glass (Samsung, 2011). This technique would eliminate optical loss inside the LED case.

Another option is to change the materials inside the case. A denser gas may transfer heat better to the case and provide a better optical path through the window with a reduced reflection coefficient. A downside is that a denser gas may dissipate or absorb the UV light. A dielectric fluid may absorb some light as well but it has the potential to transfer a significant amount of heat. Yet another option may be to use an epoxy, similar to visible LEDs. A negative attribute of epoxies is that they are not UV resistant and yellow with exposure (Lin, 2009). Epoxies may also insulate the substrate, so a heat sink would have to be incorporated.

An improvement to the UV LED window can be made. An anti-reflective film can be installed on the inside of the window. Thin films have been shown to increase transmission over 90% in a specific UV (+10 nm) range (Vaillant, 2010) and over the entire UV range, 120 to 300 nm (Hamden, 2011).

To maximize the UV emission through the LED window the photons should be directed from the substrate. This would be possible by mounting a reflecting surface from the substrate to the lens at an incidence angle into the lens which would decrease the internal reflection angle inside the LED case. This reflector can be composed of laboratory-grade aluminum with extremely high reflectivity without regard to oxidation if the LED case is sealed with nitrogen gas or in a vacuum, as shown in Figure 26. Industry has also shown promise of using other reflective materials on which to print the substrate

which increases optical output and heat transfer, such as copper (Lau et al, 2011). The case material could also be changed to aluminum or another more reflective material. Oxidation would not be a concern if the inside is filled with an inert substance.

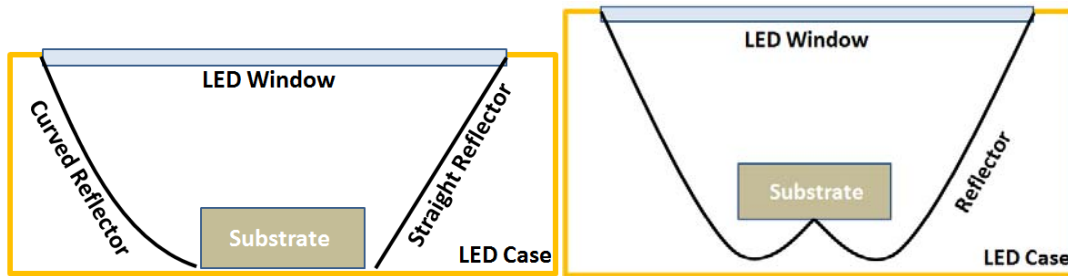


Figure 26. Potential reflectors for inside the LED

As the LED technology matures, so will the characterization of the output geometry. The initial angle defined in this research is one piece which can help create a more effective vessel. Further study should define the output in terms of wavelength shape and magnitude. When viewed on a computer, the images taken for the output angle measurements show different shades of green, blue, and purple at different intensities, meaning that different wavelengths and magnitudes of photons are interacting with the quantum dot sheet. Unfortunately, there is not a defined color scheme for wavelength with this sheet and, therefore, unable to better characterize the photons. Captain John Richwine's thesis was successful in creating a computer model which predicts the normalized output intensity. Figure 27 shows a cross-section for LED output intensity in water (Richwine, 2014).

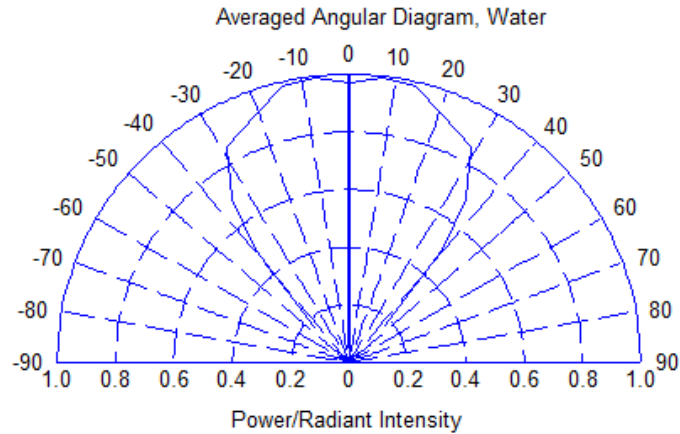


Figure 27. Example modeled cross-section of UV LED output dispersion in water; angle in degrees, intensity normalized (Richwine, 2014)

Richwine's (2014) thesis also fashioned three-dimensional depictions for the single and seven LED arrangements inside a three-inch reflective pipe, show in Figure 28. These particular plots assumed an LED output of $567 \mu\text{W}$, which is significantly greater than what is currently commercially available. Note that the drastically overpowered single LED output barely touches the edge of the three-inch container and the seven LED arrangement definitely reflects off the vessel interior surfaces and fills the space quite well. The model also plainly shows the gaps between LED conical output patterns where the UV light does not pass (Richwine, 2014). The volume between output cones should be eliminated and the size of the vessel should be scaled to the desired optical output in future vessel designs.

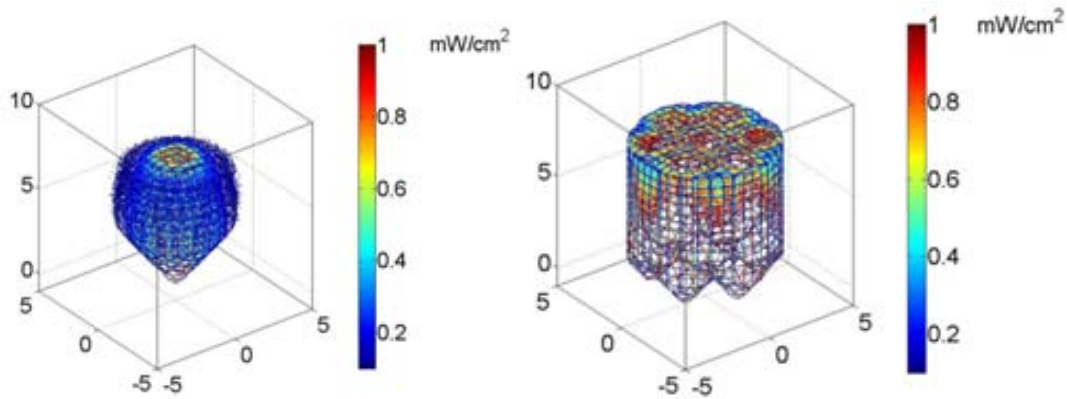


Figure 28. Modeled LED output inside a three inch reflective pipe vessel (Richwine, 2014).

Future considerations for the reactor vessel design would have the most variables to incorporate. First, a practical flow through system would require a design to keep the LED lens clean. Possible solutions include a wiper system, such as in the Aquionics large flow system, or create water turbulence to prevent sediment build-up (Spelph, 2008). Figure 29 shows a single source vessel with turbulent design. Secondly, there is a potential for a multiple LED array to compensate for the lack of power. The UV LEDs can be arranged so the emission patterns interlock, as shown in Figure 30. This pattern would be effective in a square pipe design.

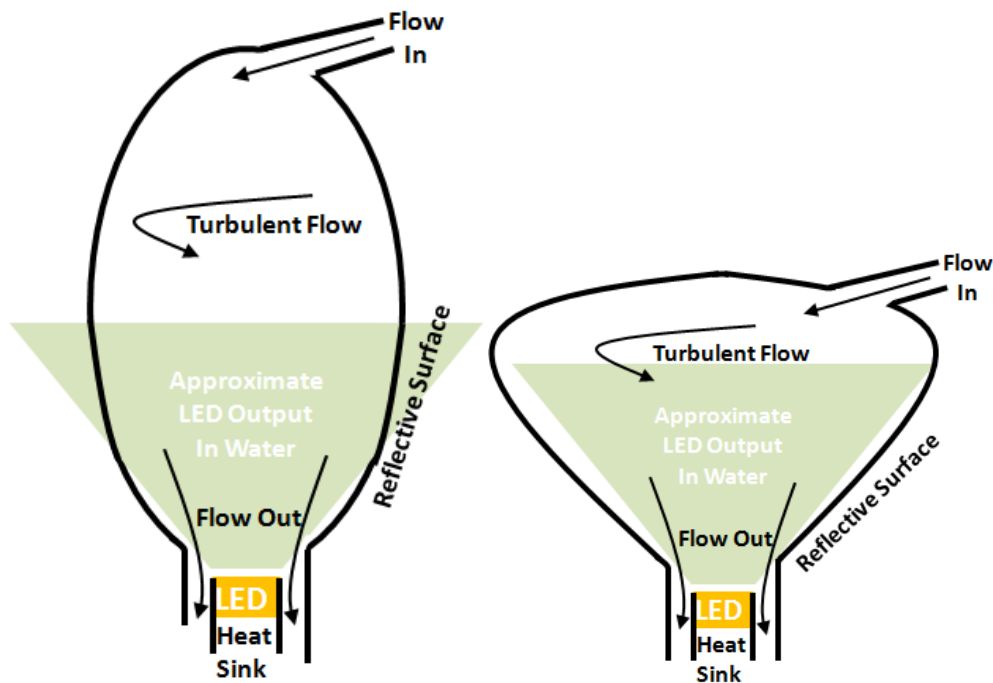


Figure 29. Single source flow through reactor vessel cross-section

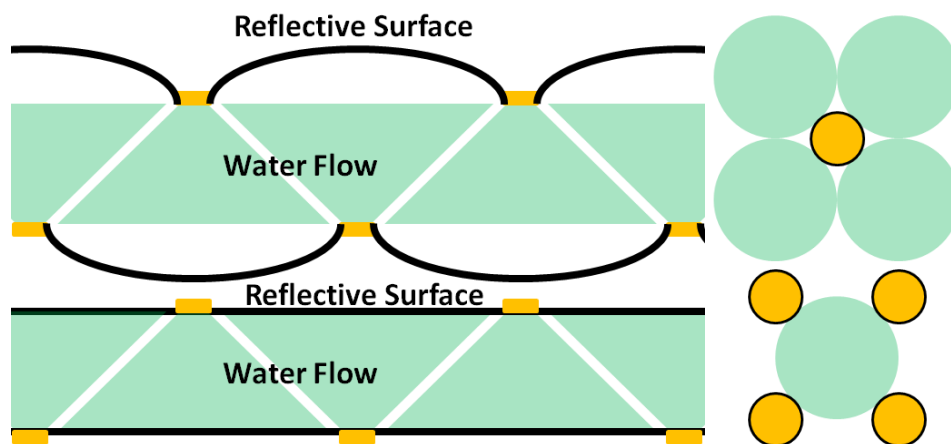


Figure 30. Multiple LED arrangement with interlocking emission patterns

Future research could also develop a better material arrangement for reflection inside the vessel. One possible solution would be to create the vessel shape out of a material that passes UV wavelength light very well, like fused silica (Newport, 2013),

and then wrap the vessel with a highly reflective metal foil, such as aluminum or molybdenum, per Table 4. A practical example could be a fused silica flask, with an angle similar to the LED output angle, similar to the shape in Figure 29. LED temperature can be controlled with the vessel design as well. A heat sink can be built into the device below the LED such that the water flow extracts heat from the LED.

Bridging from the laboratory to a practical application will be a hurdle because the laboratory measurements were conducted with deionized water which is not filled with particulates that absorb UV energy. Further research needs to identify the difference between the performance of this reactor with various levels of sediment and other sources of particulates and methods to overcome it.

Future control systems should incorporate more performance feedback. The most effective, but most technologically complex, feedback system would incorporate an optical power sensor. Until the technology matures to the point that each LED provides a predictable amount of power, continuous measuring of each LED would enable the system to compensate for an LED that is under- or over-performing. This would ensure that the system is providing an adequate UV dose and simultaneously not wasting energy. One possible solution is a fiber optic cable aimed directly at the LED which sends a signal to an UV measuring device. A back-up system for dose monitoring could be a water quality or contaminant monitoring system.

Control systems should be a critical research area. At this point, it is unknown if another pulse shape is more effective at interacting with water. More specifically, the other researchers utilized a square wave, but another wave drive, such as triangular, may be more effective. Furthermore, pulsing the current from 0 mA to peak may not be as

effective as pulsing from a floor value, such as 10 mA, to peak value, effectively having a constant current and pulse drive running simultaneously, as shown in Figure 31. Lastly, future research should quantitatively study the effect of duty cycle and pulsing intensity on life span and temperature since they are linked.

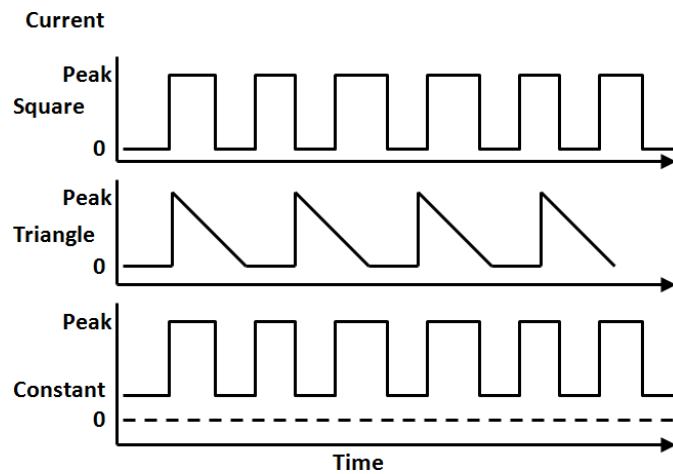


Figure 31. Square wave, triangular, and square pulse with constant current

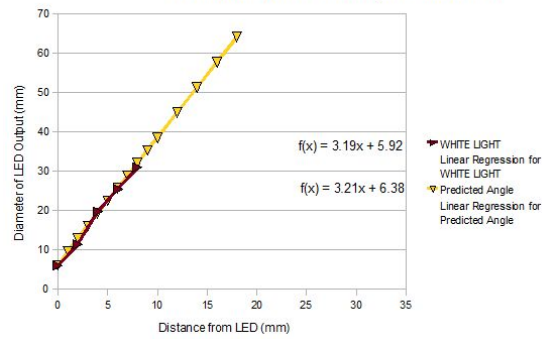
Recommendations for Action

UV LED technology is still in its infancy and we require more fundamental research to identify all variables in the system. As effective attributes are identified, each one should be independently tested. For instance, the aforementioned effect of an effective duty cycle and pulsing intensity on the LED lifespan and temperature should be studied with specific measurements of heat flow. Experiment design encompassing all of the variables should mature as the industry produces more powerful and effective UV LED bulbs. The next step of experiments could use the existing equipment to measure the electronic control variables; pulse shape, intensity, and drive frequency. For

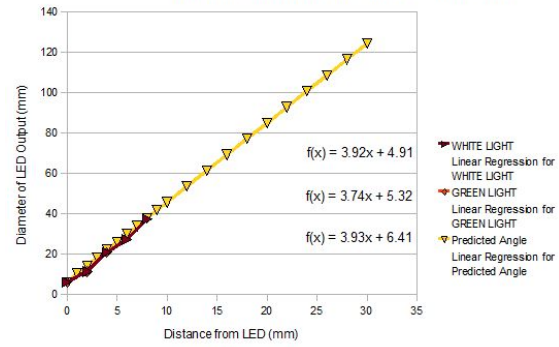
experiments that require more precise observations of dose and efficacy, a new reactor vessel following the previous recommendations should be constructed.

APPENDIX: LED OUTPUT ANGLE PLOTS

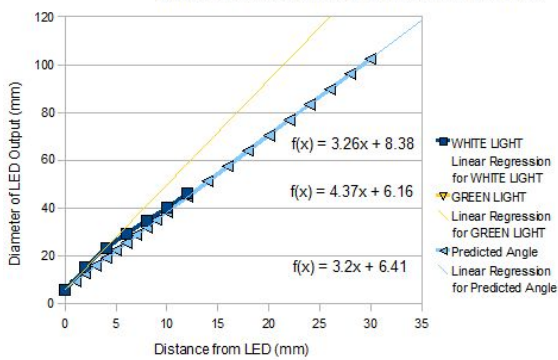
Diameter of 240 nm LED Output at 30 mA in air



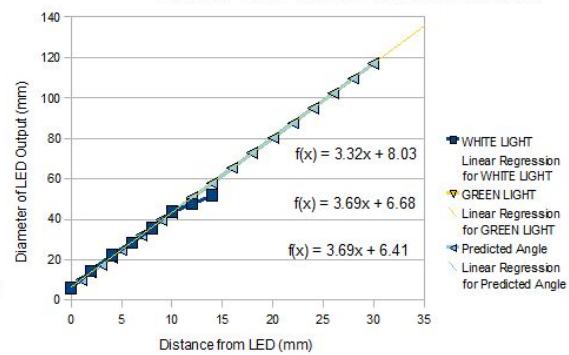
Diameter of 240 nm LED Output at 40 mA in air



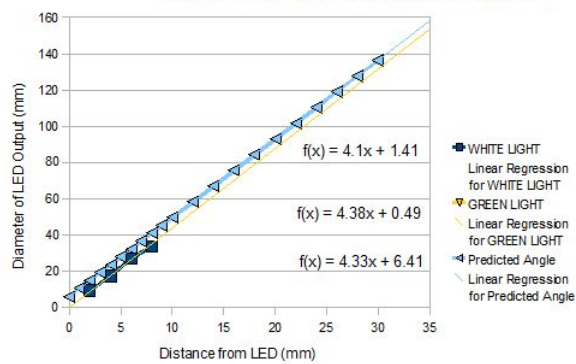
Diameter of 260 nm LED Output at 20 mA in air



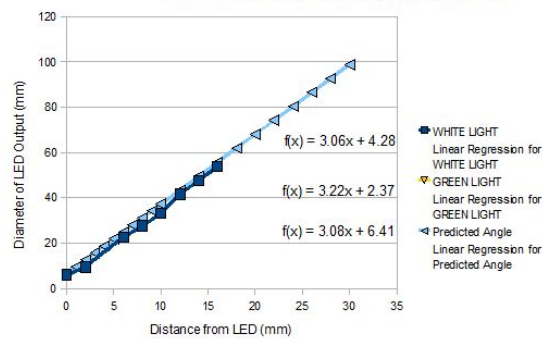
Diameter of 260 nm LED Output at 30 mA in air

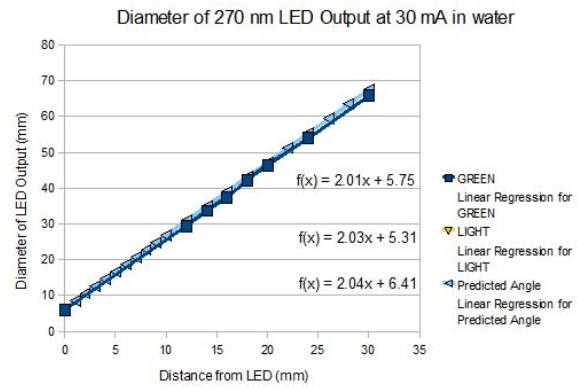
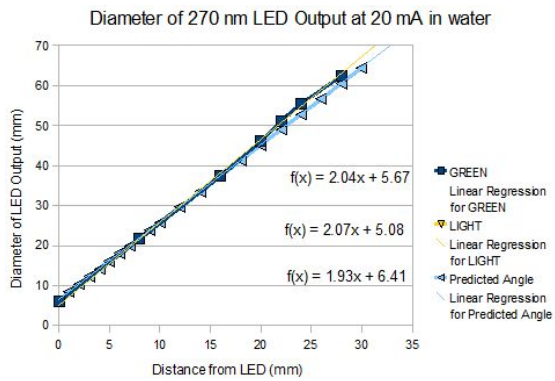
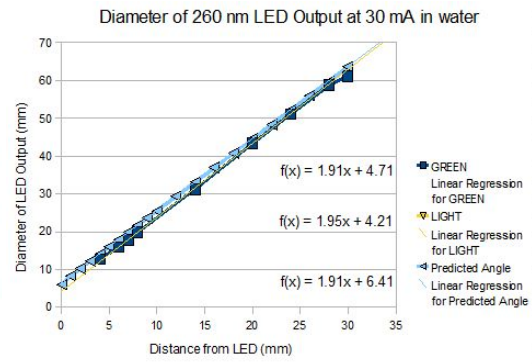
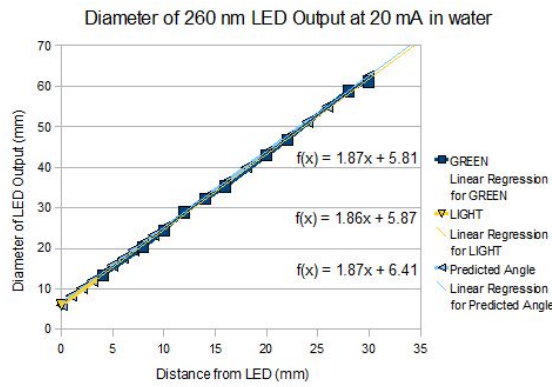
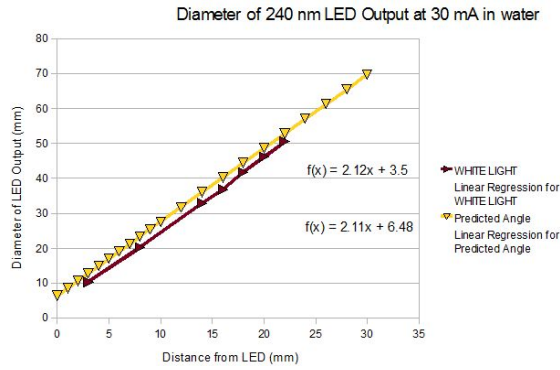


Diameter of 270 nm LED Output at 20 mA in air



Diameter of 270 nm LED Output at 30 mA in air





BIBLIOGRAPHY

- Aquionics, 2012. “Drinking Water Overview.” <http://www.aquionics.com/main/uv-applications/municipal/drinking-water/> Accessed 01 November 2012.
- Aquionics, 2013. “UV-Pearl.” <http://www.aquionics.com/main/uv-pearl/> Accessed 13 March 2013.
- Bates, Christopher. “Ultra Violet Light Emitting Diode Optical Power Characterization.” Draft. Air Force Institute of Technology, 2014.
- Bolton, J.R., Linden, K.G., 2003. Standardization of methods for fluence (UV dose) determination in bench-scale UV experiments. *Journal of Environmental Engineering* 129 (3), p209–215.
- Chevremont, A.-C., Boudenne, J.-L., Coulomb, B., Farnet, A.-M., “Impact of watering with UV-LED-treated wastewater on microbial and physico-chemical parameters of soil,” *Water Research* (2013), doi: 10.1016/j.watres.2013.01.006.
- Daimon, Masahiko and Masumura, Akira, 2007. “Measurement of the refractive index of distilled water from the near-infrared region to the ultraviolet region” *Applied Optics*, Vol. 46, Issue 18, pp. 3811-3820 (2007)
<http://dx.doi.org/10.1364/AO.46.003811>
- Davidson, Michael. “Fundamentals of Light Emitting Diodes.” Carl Zeiss Microscopy Online Campus. <http://zeiss-campus.magnet.fsu.edu/print/lightsources/leds-print.html> Accessed 8 November 2013.
- Duckworth, Kelsey. “Ultraviolet Light Emitting Diode Use in Advanced Oxidation Processes.” Draft. Air Force Institute of Technology, 2014.
- Electro-Polish. 332 Vermont Ave. Dayton, Ohio 45404. 937-222-3611
<http://www.electro-polish.com/processes/electropolish/>
- Fodor, F., 1999. “The Densest Packing of 19 Congruent Circles in a Circle.” *Geom. Dedicata* 74 (1999), p139–145.
- Fodor, F., 2000. “The Densest Packing of 12 Congruent Circles in a Circle.” *Beiträge zur Algebra und Geometrie, Contributions to Algebra and Geometry* 41 (2000), p401–409.
- Graham, R.L. “Sets of points with given minimum separation” (Solution to Problem E1921), *Amer. Math. Monthly* 75 (1968) p192-193.

- Hamden, Erika; Greer; Hoenk, Michael; Blacksberg, Jordana; Dickie, Matthew; Nikzad, Shouleh; Martin, Christopher; Schiminovich, David. "UV Anti-Reflection Coatings for Use in Silicon Detector Design." Draft. Columbia University, 2011.
- Hecht, Eugene. "Optics Fourth Edition." Addison Wesley, San Francisco, CA. 2002.
- Lenk, Ron; Lenk, Carol. "Practical Lighting Design with LEDs." Wiley-IEEE Press, Hoboken, New Jersey. 2010.
- Lin, Chih-hau; Li, Hsun-Tien; Huang, Shu-Chen; Hsu, Chia-Wen; Chen, Kai-Chi; Chen, Wen-Bin. "Development of UV Stable LED Encapsulants." Microsystems, Packaging, Assembly and Circuits Technology Conference, 2009. IMPACT 2009. 4th International, 21-23 October, 2009.
- McMaster, 2013. www.mcmaster.com. Cleveland, OH.
- NANACO Group PLC. "Quantum Dots – Background Briefing." <http://www.nanocotechnologies.com/content/AboutUs/AboutQuantumDots.aspx> Accessed February 4, 2014.
- Newport Corporation, 2013. "Optical Materials." <http://www.newport.com/Optical-Materials/144943/1033/content.aspx> Accessed 24 April 2013
- Palik, Edward D. (1978). Handbook of Optical Constants of Solids. Academic Press, Inc, San Diego, CA. 1978.
- Palik, Edward D. (1991). Handbook of Optical Constants of Solids II. Academic press, Inc, San Diego, CA. 1991.
- Perry, Karl. "Optimizing LED Lighting Systems for Efficiency, Size and Cost." *Power Electronics Technology*. January 2011, p29.
- Refractive Index Database. <http://refractiveindex.info/?group=LIQUIDS&material=Water> Accessed 19 May 2013
- Richwine, John. "Modeling Ultraviolet Light Emitting Diode Energy Propagation in Reactor vessels." Draft. Air Force Institute of Technology, 2014.
- Samsung. "GaN LED realized on a glass substrate for the first time in the world." <http://www.sait.samsung.co.kr/saithome/AboutView.do?method=get&newSeq=1032> Published 11 October 2011. Accessed 6 February 2014.
- Sensor Electronic Technology, Inc (S-ETi). "Deep UV Technical Catalogue." 2011.

- Sensor Electronic Technology, Inc (S-ETi). "Quality Control Inspection Report." Part Order Number 030813DL. 26 March 2013.
- Spelph. "Aquionics Promo Video." <http://www.youtube.com/watch?v=2dAQMsBgLYE> Uploaded 17 October 2008. Accessed 1 November 2012.
- Spectralight, 2013. "Spa and Hot Tub Ultraviolet Systems." <http://www.spectralightuv.com/hot-tub-spa-uv-systems.html> Accessed 13 March 2013.
- Standish, Ben. "LEDs for Bioanalytical and Medical Instruments." Bookham, Inc. <http://www.photonics.com/Article.aspx?AID=37678> Accessed 5 February 2014.
- Superbrightleds. "DynaOhm Driver, 2 Lead Constant Current Resistor." <http://www.superbrightleds.com/moreinfo/component-led-accessories/led-resistor-dynaohm-dc-constant-current/1054/> Accessed 5 February 2014
- Taniyasu, Yoshitaka; Kasu, Makoto; Makimoto, Toshiki. "An aluminium nitride light-emitting diode with a wavelength of 210 nanometres." NTT Basic Research Laboratories, NTT Corporation, 3-1 Morinosato-Wakamiya, Atsugi, 243-0198, Japan. 2005.
- Tran, Tho. "Comparison of Continuous Versus Pulsed Ultraviolet Light Emitting Diode Use in Water Disinfection on Bacillus Globigii Spores." Draft. Air Force Institute of Technology, 2014.
- Vaillant, Joel; Grand, Gilles; Lee, Yann; Raby, Jacques; Cazaux, Yvon; Henrion; Hibon, Vincent. "High Performance UV Anti-Reflection Coating For Back Thinned CCS and CMOS Image Sensors." e2V semiconductors, Saint-Egreve Cedex, France. Paper as presented at the International Conference on Space Optics, 4-8 October 2010.
- Watts, M. and Linden, K. "Photooxidation and subsequent biodegradability of recalcitrant tri-alkyl phosphates TCEP and TBP in water." Published online 1 October 2008. Elsevier Ltd, 2008.

REPORT DOCUMENTATION PAGE				Form Approved OMB No. 074-0188	
<p>The public reporting burden for this collection of information is estimated to average 1 hour per response, including the time for reviewing instructions, searching existing data sources, gathering and maintaining the data needed, and completing and reviewing the collection of information. Send comments regarding this burden estimate or any other aspect of the collection of information, including suggestions for reducing this burden to Department of Defense, Washington Headquarters Services, Directorate for Information Operations and Reports (0704-0188), 1215 Jefferson Davis Highway, Suite 1204, Arlington, VA 22202-4302. Respondents should be aware that notwithstanding any other provision of law, no person shall be subject to a penalty for failing to comply with a collection of information if it does not display a currently valid OMB control number.</p> <p>PLEASE DO NOT RETURN YOUR FORM TO THE ABOVE ADDRESS.</p>					
1. REPORT DATE (DD-MM-YYYY) 27-03-2014		2. REPORT TYPE Master's Thesis		3. DATES COVERED (From – To) Aug 2012 – Mar 2014	
TITLE AND SUBTITLE Design Considerations for a Water Treatment System Utilizing Ultra-Violet Light Emitting Diodes				5a. CONTRACT NUMBER	
				5b. GRANT NUMBER	
				5c. PROGRAM ELEMENT NUMBER	
6. AUTHOR(S) Spencer, Michael J., Captain, USAF				5d. PROJECT NUMBER	
				5e. TASK NUMBER	
				5f. WORK UNIT NUMBER	
7. PERFORMING ORGANIZATION NAMES(S) AND ADDRESS(S) Air Force Institute of Technology Graduate School of Engineering and Management (AFIT/ENY) 2950 Hobson Way, Building 640 WPAFB OH 45433-8865				8. PERFORMING ORGANIZATION REPORT NUMBER AFIT-ENV-14-M-58	
9. SPONSORING/MONITORING AGENCY NAME(S) AND ADDRESS(ES) US Environmental Protection Agency ATTN: Matthew Magnuson 25 W. Martin Luther King Dr. Mailstop NG-16 Cincinnati, OH 45268 (513)569-7321, magnuson.matthew@epa.gov				10. SPONSOR/MONITOR'S ACRONYM(S) EPA	
				11. SPONSOR/MONITOR'S REPORT NUMBER(S)	
12. DISTRIBUTION/AVAILABILITY STATEMENT DISTRIBUTION STATEMENT A. APPROVED FOR PUBLIC RELEASE; DISTRIBUTION UNLIMITED.					
13. SUPPLEMENTARY NOTES This material is declared a work of the U.S. Government and is not subject to copyright protection in the United States.					
14. ABSTRACT UV LED technology is in its infancy and research as it applies to UV water treatment is required to advance knowledge for practical application. This thesis focused on two subjects. First, the design, fabrication, and operation of a water treatment reaction system utilizing Ultra-Violet (UV) Light Emitting Diodes (LEDs). Second, the measurement of UV LED output angle in water which is necessary to support future reactor designs. Several characteristics of the LED-water interface were revealed which impacted the effectiveness of the vessel including; UV dose requirements, LED wavelength, photon dispersion geometry, LED placement, optical efficiency, vessel material, and electronic control system. The reactor vessel design balanced optimal characteristics with experiment design flexibility, fabrication speed, and procurement considerations. Expedient construction was required to permit laboratory exploration performed by other researchers studying bacterial spore disinfection, an advanced oxidation process, and UV LED output wavelength and intensity observations. Two reactor vessels and three electronic boards were completed and modified as the research matured. Next, the UV LED output angle in air and water was measured. The conclusions of the literature review, practical application, and output angle calculations led to future design considerations for a UV LED, water reaction vessel, and electronic control system.					
15. SUBJECT TERMS Ultra Violet, Light Emitting Diode, Water Disinfection, Reactor Vessel					
16. SECURITY CLASSIFICATION OF:			17. LIMITATION OF ABSTRACT UU	18. NUMBER OF PAGES 75	19a. NAME OF RESPONSIBLE PERSON Michael E. Miller, AFIT/ENV
a. REPORT U	b. ABSTRACT U	c. THIS PAGE U			19b. TELEPHONE NUMBER (Include area code) (937) 255-6565, ext 4651 (NOT DSN) (Michael.miller@afit.edu)